Journal of Medicinal Chemistry Article

J. Med. Chem. **2010,** *53,* 759–777 **759**
DOI: 10.1021/jm9014263

Hit to Lead Account of the Discovery of Bisbenzamide and Related Ureidobenzamide Inhibitors of Rho Kinase

Tina Morwick,*,† Frank H. Büttner,‡ Charles L. Cywin,† Georg Dahmann,‡ Eugene Hickey,† Scott Jakes,† Paul Kaplita,† Mohammed A. Kashem,† Steven Kerr,† Stanley Kugler,† Wang Mao,† Daniel Marshall,† Zofia Paw,† Cheng-Kon Shih,† Frank Wu,† and Erick Young†

†*Boehringer Ingelheim Pharmaceuticals, Inc., 900 Ridgebury Road, Ridgefield, Connecticut 06801-0368, and* ‡*Boehringer Ingelheim Pharma GmbH and Co. KG, Birkendorfer Strasse 65, D-88397 Biberach an der Riss, Germany*

Received September 24, 2009

A highly selective series of bisbenzamide inhibitors of Rho-associated coiled-coil forming protein kinase (ROCK) and a related ureidobenzamide series, both identified by high throughput screening (HTS), are described. Details of the hit validation and lead generation process, including structure−activity relationship (SAR) studies, a selectivity assessment, target-independent profiling (TIP) results, and an analysis of functional activity using a rat aortic ring assay are discussed.

Introduction

The evolution from a pharmacology-based to a target-based approach in drug discovery has presented both opportunities and challenges to the pharmaceutical industry.[1] Utilization of high-throughput biochemical assays for the identification of small molecule chemical ligands which interact with distinct protein targets greatly enhances the ability to identify potential drug candidates, and knowledge of the specific molecular target provides information to support mechanism of action. Significant challenges exist, however, in the identification of druggable, disease-relevant targets, and the selection of biochemically active lead structures which can be developed into pharmacologically active agents useful in the treatment of disease. When high-throughput screening (HTS)[a] enables the target-based lead identification (LI) process, hit-to-lead (HtL) groups have been utilized.[2] This core LI group facilitates the validation of screening hits and selection of promising lead candidates. In this paper, we describe our HtL efforts to identify inhibitors of Rho kinase and our discovery of a series of bisbenzamides and related ureidobenzamides as novel chemotypes demonstrating potent Rho kinase inhibition.

Rho kinase, also referred to as Rho-associated coiled-coil containing serine/threonine protein kinase (ROCK) is a downstream effector of RhoA G proteins following GTP-binding and activation. In humans, the Rho family consists of at least 20 members and belongs to the Ras superfamily of monomeric GTP/GDP-binding (GTP)ases.[3] Rho A, one of the most well-characterized members, was originally identified as a homologue to oncogene Ras.[4] RhoA influences multiple cellular processes including cytoskeletal rearrangement, gene expression, and membrane trafficking, as well as cell adhesion, migration, differentiation, proliferation, and apoptosis.[5] The name Rho sometimes refers collectively to RhoA, RhoB, and RhoC, which share identical effector domains, and Rho kinases bind to all three.[6] A member of the AGC family of protein kinases, ROCK plays a key role in regulation of smooth muscle contraction and formation of stress fibers and focal adhesions in nonmuscle cells.[7] Two Rho kinase isoforms have been identified, ROCK1 and ROCK2, which share 65% overall homology with 92% identity in their kinase domains and absolute identity in the ATP-binding pocket.[4b] These proteins are ubiquitously expressed, but ROCK1 is reportedly more prominent in lung, liver, and testes, while ROCK2 expression is enriched in brain and muscle.[4b,8] ROCK1 and ROCK2 have generally been considered to be functionally redundant. However, sporadic reports have highlighted some differences.[9] For example, studies with primary rat embryo fibroblasts have suggested that stress fiber and focal adhesion formation may be dependent on ROCK1 but not ROCK2. Also, it has been noted that ROCK1, but not ROCK2, binds and phosphorylates RhoE.[10] A unique function for ROCK2 in mediating glucocorticoid-induced formation of tight junction sealing in rat mammary epithelial cells has also been reported. This apparently occurs as a consequence of differential expression and activity of Rho kinase isoforms following treatment with dexamethasone.[11]

A key mechanism for regulation of muscle cell contractility and nonmuscle cytoskeletal organization through the Rho/ROCK pathway involves the phosphorylation state of the molecular motor myosin II on Ser19 of its regulatory light chain (MLC). Phosphorylation of this residue leads to increased contractility and formation of stress fibers and focal adhesions. Maintaining Ser19 of MLC in a phosphorylated state is accomplished by protein kinases such as myosin light

*To whom correspondence should be addressed. Phone: (203) 798-5751; Fax: 203-798-5297. E-mail: tmorwick@rdg.boehringer-ingelheim.com.

[a] Abbreviations: AGC, cAMP-dependent, cGMP-dependent and protein kinase C; CDC42BPB, CDC42-binding protein kinase β; DMPK, dystrophia myotonica protein kinase; GDP, guanosine-5′-diphosphate; GTP, guanosine-5′-triphosphate; HTS, high-throughput screening; HtL, hit-to-lead; IMAP, immobilized metal ion affinity-based fluorescence polarization; ITC, isothermal titration calorimetry; LHS, left-hand side; LI, lead identification; MBS, myosin binding subunit; MLC, myosin light chain; MLCK, myosin light chain kinase; MLCP, myosin light chain phosphatase; PI3K, phosphatidylinositol 3-kinase; PKA, protein kinase A; PKN2, PKC-related kinase, protein kinase N2; PKCε, protein kinase C epsilon; POC, percent of control; RBD, Rho binding domain; RHS, right-hand side; SCX, strong cation exchanger, silica-bound *p*-toluenesulfonic acid; *Si*-DMA, silica-bound dimethylamine; TF, tissue factor.

Published on Web 12/10/2009

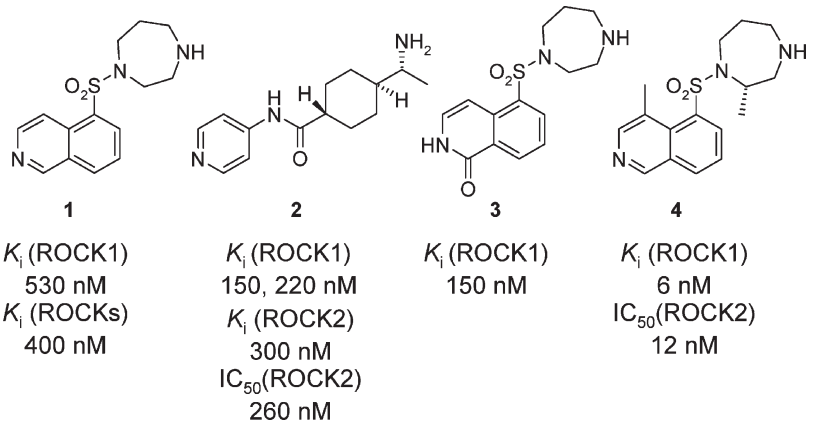

Figure 1. Literature benchmark Rho kinase inhibitors with X-ray structures. ROCK1 data reported in refs 25 and 26a. ROCK2 data reported in refs 25 and 34a.

chain kinase (MLCK) through a Ca^{2+}-dependent mechanism and inhibition of myosin light chain phosphatase (MLCP) via a Ca^{2+}-independent process. Activated ROCK inhibits MLCP by phosphorylation of its regulatory myosin binding subunit (MBS), thereby prolonging the phosphorylated state of MLC at serine 19. Additionally, ROCK can reportedly directly phosphorylate MLC.[4a,4b,12]

The Rho/ROCK pathway is activated by multiple stimuli including various GPCR agonists and inflammatory cytokines. ROCK activity is self-regulated by an autoinhibitory carboxy terminus. The C-terminal region incorporates a Rho-binding domain and the interaction between RBD and Rho-GTP reverses autoinhibition and activates the kinase. This autoinhibitory region also contains a pleckstrin homology domain, which may have a regulatory role by interaction with lipid mediators, and lipids such as arachidonic acid have been found to activate Rho kinase.[4b,13]

Multiple potential therapeutic opportunities have been suggested for Rho kinase inhibitors including cardiovascular and cerebrovascular conditions such as hypertension, heart failure, angina, myocardial infarction, atherosclerosis, coronary and cerebral vasospasm and stroke,[4a,4b,6a,6b,14] neurological disorders including Alzheimer's disease, multiple sclerosis, spinal cord injury, and neuropathic pain,[15] osteoporosis,[16] cancer,[17] bronchial asthma,[18] and glaucoma.[19] Our interest in Rho kinase was associated with its role in cardiovascular function. Both Rho and ROCK are ubiquitously expressed in vascular cells including smooth muscle, endothelial, cardiac myocytes, platelets, leukocytes and monocytes/macrophages,[4b] and inhibition of Rho kinase in animal models of cardiovascular disease has demonstrated positive results in a variety of the pathological conditions cited above.[20] Additionally, certain endogenous agents or xenobiotics associated with positive cardiovascular outcomes may derive some of their benefit through moderation of Rho/ROCK signaling. For example, down-regulation of Rho kinase expression has been associated with physiological concentrations of estrogen, and Rho/ROCK activity has also been found to inversely correlate with eNOS expression and NO availability.[20,21] The cardiovascular benefits of HDL also may result in part from inhibition of thrombin-induced tissue factor (TF) upregulation via inhibition of RhoA and stimulation of PI3K.[22] Statins have demonstrated clinical benefits in cardiovascular disease beyond their cholesterol-lowering effect. These so-called pleiotropic or cholesterol-independent effects may be mediated by reduction of isoprenoid metabolites required for post-translational protein prenylation and membrane targeting, an essential mechanism for activation of RhoA.[23]

Table 1. Counterscreens Used for Triaging ROCK2 Actives

kinase	% ID[a]
PKCε	39
DMPK	50
CDC42BPB	53
PKN2	34

[a] Sequence ID to ROCK2 (kinase domain).

Several ROCK inhibitors have been reported in the literature, and many are summarized in a recent review.[24] Benchmark compounds used extensively to investigate the functional outcome of Rho kinase inhibition include fasudil (HA-1077, **1**) and Y-27632 (**2**). Fasudil is the only marketed Rho kinase inhibitor approved in Japan for treatment of cerebral vasospasm after subarachnoid hemorrhage.[24a] Fasudil undergoes oxidation in vivo to isoquinolinone **3** (hydroxyfasudil), which is equipotent,[25] and a dimethyl analogue (H-1152P, **4**) shows improved potency. X-ray crystal structures of **1**−**4** in complex with ROCK1 dimer have been published (Figure 1).[26]

Results and Discussion

HTS Assay and Hit Validation Results for Inhibitor 5. The corporate compound collection was screened in a homogeneous luciferase assay using ROCK2 (1−543), substrate AKRRRLSSLRA, and a luciferin-luciferase detection reagent to quantify residual ATP. Dose−response data on compounds showing reproducible activity from the screen was generated for ROCK2 using the same assay format. Selectivity data was acquired simultaneously on the ROCK2 actives utilizing four proteins which were selected for counterscreening (rule-out) based on sequence homology (DMPK, CDC42BPB), chemotype sensitivity (PKN2), and functional significance (DMPK, PKCε, Table 1). Hits of interest were also evaluated for ROCK1 potency, and our objective at the time was the identification a dual inhibitor.

Generic criteria for hit validation has been recently published.[27] One series which passed the initial filtering exercise is exemplified by the bisbenzamide structure **5** (Figure 2). This hit demonstrated low micromolar potency for both ROCK1 and ROCK2 in the luciferase assay and comparable functional activity in our aortic ring assay, which was somewhat surprising assuming an ATP competitive mechanism of

inhibition. One attraction of **5** was the bisbenzamide motif, which is unusual in comparison to known kinase inhibitors, and we speculated that the scaffold might offer some advantage toward achieving selectivity. Compound **5** was not active in the counterscreen assays (all >5 μM), but its relatively weak potency for Rho kinase provided a small window for selectivity assessment. Evaluation of physicochemical properties and in vitro pharmacokinetic and safety parameters for **5** is shown in Table 2. The inhibitor had good aqueous solubility but poor metabolic stability, and our Caco-2 results suggested that permeability may be compromised by transporter-mediated efflux. The compound also showed moderate inhibition of CYPs 2C9 and 3A4. This assessment identified areas which would need to be addressed during the lead generation stage.

Lead Generation: SAR Studies. Compound **5** and additional related actives having similar potency were identified from the screen. An analogous series of ureidoarylamides was also found, and some examples from both series are shown in Figure 3. Because no crystal structure for Rho kinase was available at the time of our studies, a computational model was developed based on a crystal structure of PKA, another member of the AGC subfamily (37% homology with ROCK2, kinase domain), in complex with the Rho kinase inhibitor **1** (PDB code: 1Q8W).[28] Docking studies of **5** and related bisbenzamides were not conclusive, and several ligands including **5** did not dock using a hinge-binding interaction as a required constraint. Studies with ligands for which a binding hypothesis could be identified suggested the ligand may form a hydrogen bond interaction with hinge region residue Met172 (NH) via the pyridine nitrogen. Known Rho kinase inhibitors utilize a variety of residues for hydrogen bonding to the hinge including pyridines, quinolines, azaindoles, indazoles, amides, and ureas.[15a] However, for the bisbenzamides, a search of the screening results (actives and inactives) suggested that the dimethoxyphenyl rather than the pyridine was important for potency. For the urea series, screening data attributed significance to the cyanophenyl seen in **8** and **9**, and while the pyridine fragment was also incorporated into this hit series, the data again indicated its presence was trivial. Our initial SAR studies targeted the bisbenzamide series probing the relevance of these two terminal sites. For the dimethoxyphenyl, removal of either methoxy group, conversion to the methylenedioxy, or replacement with a dimethyl (**10**−**13**) was generally detrimental, indicating the intact LHS fragment was important for binding (Table 3). Modifications to the ethylpyridine substituent are shown in Table 4. Conversion to the constrained isoquinoline (**14**) provided a modest improvement. To assess whether the pyridine/isoquinoline nitrogen secured the hydrogen bond donor interaction from the hinge, the corresponding saturated derivatives with a basic amine replacement (**15**, **16**) were made. If the pyridine (or isoquinoline) nitrogen participated in this interaction, the

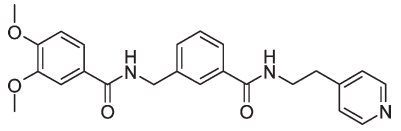

5: 2.3 μM (hROCK2); 4.3 μM (hROCK1); 1.9 μM aortic ring functional assay

Figure 2. Results for resynthesized compound **5**.

Table 3. Dimethoxyphenyl Replacements

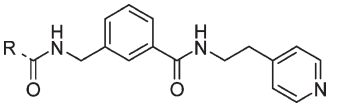

Entry	R	hROCK2 IC_{50} (nM)
10	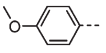	>7000
11	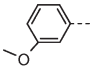	>7000
12	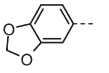	>7000
13	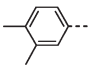	>7000

Table 2. Target-Independent Profiling Results for **5**

MW	sol[a]	Caco-2[b]	Caco-2[c]	HLM $t_{1/2}$(min)	CYP 1A2[d]	CYP 2C9[d]	CYP 2C19[d]	CYP 2D6[d]	CYP 3A4[d,e]
419	> 100/63	0.5	29.1	10	> 30	16	> 30	> 30	4/21

[a] Solubility (μg/mL) @ pH 4.5/7.4. [b] A to B $\times$ 10^{-6} cm/s. [c] B to A $\times$ 10^{-6} cm/s. [d] μM. [e] Substrates 7-benzyloxy-4-trifluoromethylcoumarine/7-benzyloxyquinoline (BFC/BQ). (See Supporting Information for method details.)

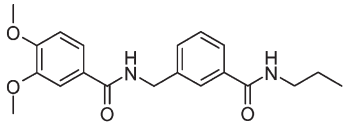

6: 5.0 μM (hROCK2)

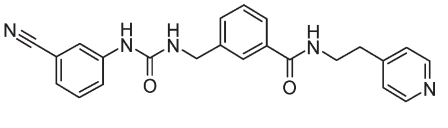

8: 5.5 μM (hROCK2)

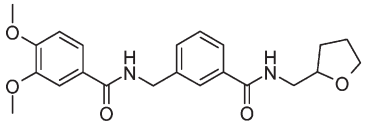

7: 1.2 μM (hROCK2)

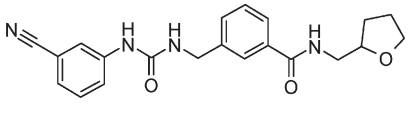

9: 3.5 μM (hROCK2)

Figure 3. Examples of bisbenzamide and ureiobenzamide actives from the screen. Compounds **7** and **9** are racemic.

Table 4. RHS Optimization

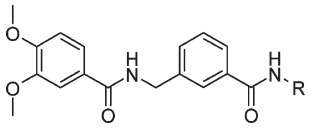

Entry	R	hROCK2 IC_{50} (nM)[a]
14	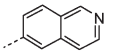	685±130
15	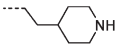	176±31
16	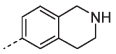	100±12
17[b]	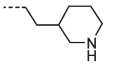	53±6.3
18	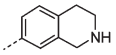	33±5.6
19[b]	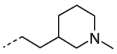	102±11
20	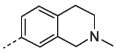	46±7.7
21	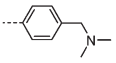	69±8.9
22	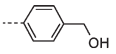	870±133

[a] Assay values reported as the mean ± SEM of $n \geq 2$ independent replicates. [b] Racemic.

corresponding basic amines should lose potency as these would be protonated and unable to accept a hydrogen bond. On the contrary, a moderate to significant improvement was observed, inconsistent with the docking hypothesis but compatible with the screening data analysis. Known Rho kinase inhibitors such as **1**−**4** also have a basic amine moiety. Having demonstrated a potentially optimizable binding interaction with a basic amine, further exploration of this area was carried out. Regioisomeric versions of **15** and **16** provided further improvement (**17**, **18**), and methylation of these analogues (**19**, **20**) was either mildly adverse (**19**) or had a negligible effect on potency (**20**). Having an aromatic ring instead of the acyclic ethyl group linking the amine fragment to the right-side amide apparently offered some advantage, albeit modest (**5** vs **14**, **15** vs **16**, **17** vs **18**). Consequently, we evaluated some substituted benzylic amines, and found the *p*-dimethylaminomethylphenyl to be optimal (**21**). These studies indicated a specific binding interaction for the basic amine. Further confirmation came from the benzyl alcohol **22**, which was expectedly less potent. ATP competition was evaluated for **15**, **16**, and **18** because these analogues provided a larger window than the hit structure **5** for observing the effects of increasing concentrations of ATP (above $K_{M,ATP}$). Using an IMAP assay format, these analogues were found to be ATP competitive, which documented a mechanism of inhibition and provided support for specific

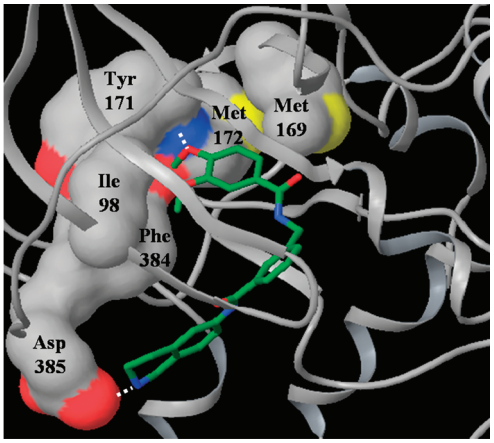

Figure 4. A partial ribbon diagram shows the binding mode for bisbenzamide **16**. Key residues (backbone and/or side chain) are shown in space-filing mode and colored by element (blue = nitrogen, red = oxygen, yellow = sulfur). Compound **16** uses the aromatic *p*-methoxy oxygen for hinge binding to Met172 (3.0 Å), while the tetrahydroisoquinoline forms an interaction with the side chain acid of Asp385 (2.6 Å). Side chain fragments for a number of hydrophobic residues in the hinge-binding region (Met169, Ile98, Phe384, and Tyr171) are also depicted.

binding to the protein. (Supporting Information). We also measured binding constants for **17** and **18** using isothermal titration calorimetry (ITC) (K_d **17** = 18 nM; K_d **18** = 7 nM). In this assay, the inhibitors demonstrated strong enthalpic binding with relative potencies consistent with the enzyme assay, which further precluded the likelihood of any nonspecific mechanism of inhibition.

Docking studies with optimized analogues featuring the basic amine moiety remained somewhat inconclusive, and again imposing the hinge-binding constraint, several structures did not dock. However, basic analogues which did provide a binding hypothesis suggested a potential hinge-binding interaction with the oxygen of the *p*-methoxy moiety in contrast to the pyridine identified earlier. This alternative binding mode is exemplified by the tetrahydroisoquinoline **16** (Figure 4). As can be seen in the figure, the *p*-methoxy oxygen of **16** forms a hydrogen bond interaction with the NH of hinge region residue Met172. The tetrahydroisoquinoline nitrogen forms an interaction with the side chain acid of Asp385. The docking hypothesis generated for **16** seemed more reliable, but taken as a whole, the evidence from modeling studies to support this hinge-binding interaction was not compelling since many structures failed to dock and we therefore used our SAR studies to further probe the binding mode of our inhibitors.

The next series of structures were designed to evaluate the linker regions. For these studies, **17** is the direct comparison. We had previously looked at methylation of the linker amides on hit structure **5** and found this to have a modest effect on potency (~2 fold reduction, data not shown). Beyond simple alkylation, most other modifications to the linker atoms resulted in a substantial to complete loss of potency as can be seen from the data in Table 5. The presence of a methylene component in the LHS linker adjacent to the central aromatic seemed important as various modifications to the 3-atom fragment which altered or eliminated this point of flexibility were not tolerated (**23**−**26**). This indicated that rotational freedom was important in this region possibly due to a bent bioactive conformation. Replacing the LHS amide

Table 5. Linker Modifications

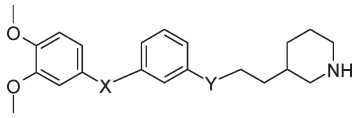

Entry	X	Y	hROCK2 IC_{50} (nM)[a]
17			53±6.3
23			>7000
24			>6000
25			3200±410
26			>6000
27			>6000
28			73±14
29			37±2.0

[a] Assay values reported as the mean ± SEM of $n \geq 2$ independent replicates.

with a sulfonamide was also detrimental (**27**). What was completely tolerated, however, was inversion of the amides (**28**, **29**). These results highlight the importance of the linker components. The amides in the linker regions were potential hinge-binding candidates, and this capacity has been associated with amide functionality in known Rho kinase inhibitors.[15a] However, the tolerance associated with reversing these fragments diminished the likelihood than these residues engaged the critical hinge-binding interaction.

We then revisited the dimethoxyphenyl fragment, and for these studies we enlisted the dimethylaminomethylphenyl RHS moiety, making **21** the direct comparison as it had good potency and offered some synthetic advantages (Table 6). Previously we had found that removal of either methoxy group from **5** resulted in inactive compounds (**10**, **11**). However, using a more potent basic amine replacement for the pyridine, we could now differentiate between the two, and found the *p*-methoxy to be somewhat more significant (**30**, **31**) as might be expected from the modeling studies. However, a considerable reduction in potency was observed on removal of either of these functional groups, affirming the importance of both. Conversion to the dihydroxy (**32**) was not tolerated nor was a methylenedioxy substitution (data not shown) as seen previously for **12**, suggesting a potential hydrophobic interaction for one or both of the methyl groups. Other replacements such as dimethyl or dichloro, or regiochemical modifications to the methoxy substituents (data not

Table 6. Modifications to the Dimethoxyphenyl Fragment

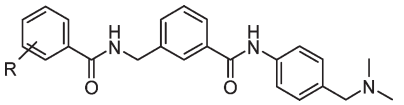

entry	R	hROCK2 IC_{50} (nM)[a]
21	3,4-diOMe	69 ± 8.9
30	3-OMe	> 7000
31	4-OMe	1300 ± 58
32	3,4-diOH	> 6000
33	3-Me-4-OMe	266 ± 61
34	3-Cl-4-OMe	92 ± 13
35	3-CF_3-4-OMe	160 ± 42
36	3-Cl-4-OCF_3	670 ± 110
37	4-CN	1700 ± 385

[a] Assay values reported as the mean ± SEM of $n \geq 2$ independent replicates.

shown), were also not tolerated. Interestingly, keeping the *p*-methoxy and substituting a methyl, chloro, or trifluoromethyl for the *m*-methoxy group recaptured some of the loss in potency (**33**−**35**), further indicating that hydrophobic interactions likely contributed to binding in this region. However the reverse tactic employing the *m*-methoxy fragment was not useful (data not shown). Because the alkoxy group at the para position consistently demonstrated its significance, we further probed its hinge-binding potential generating **36** with an electron-withdrawing trifluoromethyl bonded to the oxygen. A moderate reduction in potency was seen (7-fold) providing some support for a hinge-binding hypothesis. However, comparing **33** to **34** and **35**, it was noted that no loss in potency occurred as a result of an adjacent electron-withdrawing group as might be expected if oxygen was a hydrogen bond acceptor. We also tried to incorporate other groups at this position, which may be more capable of mediating a hydrogen bond interaction including a nitrile (**37**), amide, and urea (not shown), but nothing proved useful. While these SAR results did not clearly support the hinge-binding hypothesis suggested by docking studies, they definitively established the significance of LHS aromatic substituents for binding. Furthermore, our studies afforded some evidence to suggest that hydrophobic interactions may be important. In support of these findings, it was noted that the region occupied by these fragments in docked structure **16** (Figure 4) contained several hydrophobic residues in close proximity including Met169 (gatekeeper), Ile98, Phe384, and Tyr171.

In summary, our SAR studies for the bisbenzamide series demonstrated structure-based inhibition and identified optimizable regions. We could not determine with confidence what moiety, if any, was involved in hydrogen-bonding with the hinge. Because this is a critical feature for most kinase inhibitors, the potential absence of hinge-binding was seen as an opportunity to gain selectivity. Fragments which were deemed important included a right-hand side (RHS) aromatic linking to a saturated, basic amine moiety, the two central amide linkers, one of which incorporated an essential adjacent methylene, and the LHS aromatic attachments.

We next turned our attention to the ureidobenzamide series guided by the information acquired from the bisbenzamide work. Our starting point here focused on structure **8**, which had similar potency to hit compound **5**. Results are shown in Table 7. Replacing the pyridine of **8** with the ethylpiperidine

Table 7. SAR Studies for the Ureidobenzamide Series

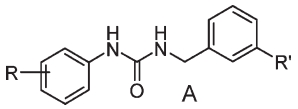

Entry	R	R'	hROCK2 IC_{50} (nM)[a]
38	3-CN	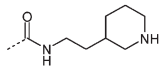	89±19
39	3,4-diOMe	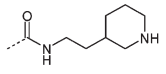	1600±418
40	4-CN	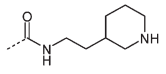	18±2.0
41	4-CN	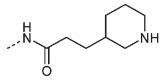	110±30
42	4-CN	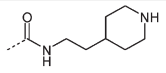	65±5.4
43	4-CN	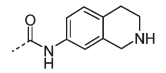	14±2.3
44	4-CN	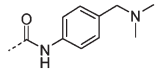	65±13
45	4-CN	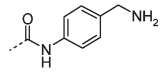	70±8.3
46	3-Cl-4-CN	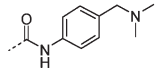	10±1.7
47	4-$C(O)NH_2$	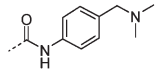	8±1.1
48	3-Cl-4-$C(O)NH_2$	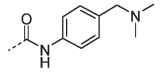	74±2.0
49	3-$C(O)NH_2$	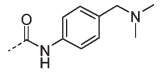	240±33
50	4-$C(O)NH_2$	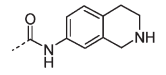	4±0.87

[a] Assay values reported as the mean ± SEM of $n \geq 2$ independent replicates.

fragment having the preferred regiochemistry led to a significant improvement in potency as seen previously (**38**). However replacement of the nitrile of **38** with the 3,4-dimethoxy pattern found optimal for the bisbenzamides had the opposite effect (**39**). This was not too surprising, as utilization of the nitrile in the bisbenzamide series also was not profitable (**37**), indicating some differences in binding for the two series. However, similar to previous findings, para substitution of the LHS aromatic contributed more significantly than meta, in this case using the nitrile substituent (**38** vs **40**). We looked at inversion of the RHS amide of **40**, an inconsequential modification in the bisbenzamide series. In this case, a moderate reduction in potency was observed (**41**). We then explored the RHS amine of **40** incorporating some of the interesting groups identified from the previous SAR. Similar regiochemical preference for the piperidine was observed comparing **42** to the preferred **40**, but incorporating the aromatic into the RHS linker had a more negligible effect on binding (**43**). A comparable tolerance was also seen for the dimethyl-substituted *p*-aminomethylphenyl analogue **44**, which was equipotent to its unsubstituted counterpart, **45**. We used the *p*-dimethylaminomethylphenyl RHS motif to further evaluate the LHS aromatic substitution. This group not only provided a synthetic advantage as before, but also, having a more moderate level of potency, it allowed us more room to quantitate improvements. Again, it was found that the substitution on the LHS aromatic was somewhat uncompromising, and most replacements for the nitrile were not tolerated. These included monosubstitution at the 3 or 4 position by methoxy, trifluoromethyl, or halogen, or a para-substituted ester or primary urea, all of which showed no inhibition up to a concentration of 5 μM (data not shown). However, incorporation of chlorine adjacent to the nitrile provided a boost in potency (**46**) as seen previously for **34**, consistently indicating the importance of hydrophobic interactions in this region. However, unlike before, on replacement of the nitrile with an amide (**47**) in an attempt to identify any hinge-binding potential for the substituent at this position, we observed an 8-fold advantage, suggesting that this series may have better access to the hinge, assuming a proximal location. Interestingly, incorporation of a chlorine substituent adjacent to the purported hinge-binding amide erased its contribution (**48**) unlike what was observed with the nitrile, suggesting these two substituents align differently to the protein. It was also noted that shifting this amide to the adjacent meta position (**49**) evoked a reduction in potency to a greater extent than seen for the nitrile. Combining the optimal RHS tetrahydroisoquinoline fragment with the preferred LHS amide substituent provided the most potent analogue **50**.

Our selection of the dimethylaminomethylphenyl motif for evaluation of LHS SAR for both the bisbenzamide and urea series led to one additional finding of interest. Some analogues incorporating this fragment demonstrated unusual inhibition curves with decreasing potency at high concentrations (above the IC_{50}), suggesting a possible solubility problem, which was not substantiated by our target-independent profiling. It was subsequently found that compounds employing this motif were in fact weak inhibiters of the luciferase enzyme used to quantify residual ATP in the assay. Increasing utilization of luminescence technology in HTS has led to an awareness of this aspect of assay interference, and an analysis of common HTS scaffolds which act as inhibitors of firefly luciferase has recently been reported.[29] We subsequently evaluated these analogues and some comparators with alternative RHS fragments using an IMAP assay and verified that the relative potencies determined from the luciferase assay were not impacted by this level of assay interference (Supporting Information).

Lead Generation: Chemistry. Standard coupling techniques were employed for synthesis of the analogues described herein. The synthesis of common intermediates **51**−**54** is

Scheme 1[a]

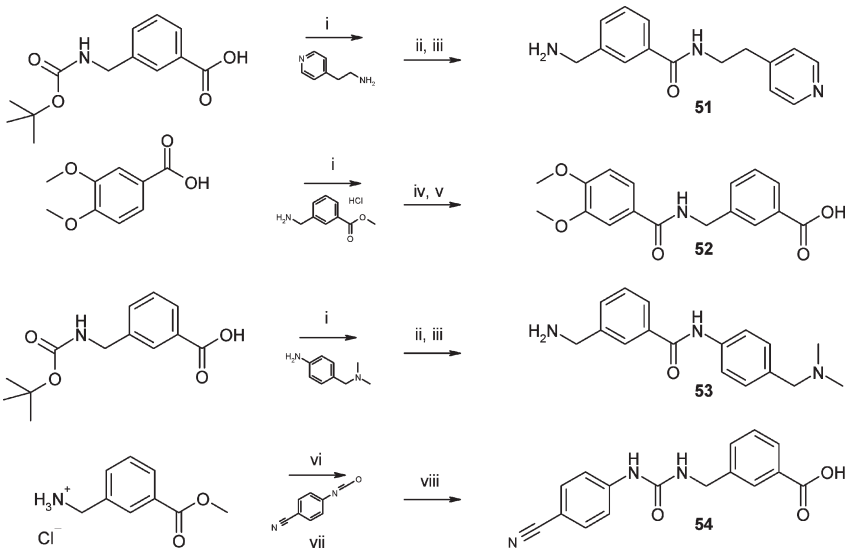

[a] (i) *N*-(3-Dimethylaminopropyl)-*N*′-ethylcarbodiimide hydrochloride, benzotriazole-1-ol, diisopropylethylamine, or *N*-methylmorpholine, DMF; (ii) SCX, dichloromethane; (iii) ammonia in methanol; (iv) Amberlyst A26 (OH^- form), methanol/DMF; (v) formic acid, methanol; (vi) *Si*-DMA, DMF; (vii) SCX; (viii) LiOH, THF, water.

Scheme 2[a]

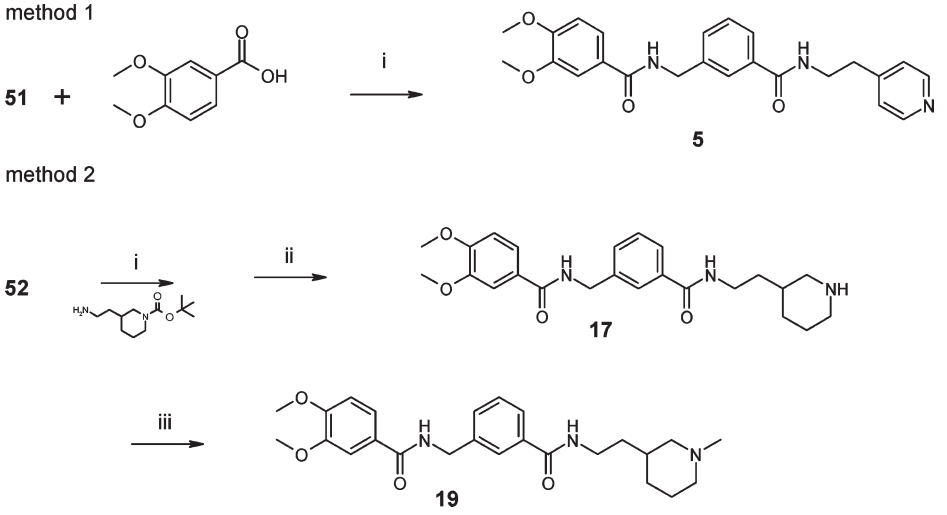

[a] (i) *N*-(3-Dimethylaminopropyl)-*N*′-ethylcarbodiimide hydrochloride, benzotriazole-1-ol, diisopropylethylamine, DMF; (ii) trifluoroacetic acid, dichloromethane; (iii) formic acid, formaldehyde.

shown in Scheme 1. Preparation of these intermediates and many of the reported analogues was facilitated by use of solid-phase reagents and scavengers including deprotection strategies incorporating catch and release technologies.[30] The general sequence for synthesis of hit compound **5** and analogues **10**−**13** (Table 3) is exemplified by method 1 (Scheme 2) demonstrating the synthesis of **5**. This directional approach, installing the RHS amide first, provided an efficient method for variation of the LHS substituents. Alternatively, initial formation of the LHS dimethoxyaryl amide fragment **52** provided a common intermediate for synthesis of analogues in Table 4. The process is exemplified by the synthesis of **17** (method 2; Scheme 2). Methylated analogues **19** and **20** were prepared from the corresponding amines using the Eschweiler−Clarke procedure.[31]

Variation of the linker region did not lend itself to utilization of common synthetic intermediates, and therefore several independent approaches to the synthesis of these analogues are exemplified in Scheme 3. Analogous couplings and deprotection strategies engaging the appropriate amine and acid fragments were employed. Standard urea formation using an aniline and arylisocyanate initiated the synthesis of **23**.

Using common intermediate **53**, analogues **30**−**37** (Table 6) were synthesized by direct coupling of an aromatic acid. Scheme 4 outlines the method exemplifying the synthesis of **30**.

Methods used for synthesis of urea analogues reported in Table 7 are outlined in Scheme 5. Synthesis of **40** was prosecuted using intermediate **54**, which was coupled to the RHS amine fragment. Deprotection provided the desired analogue. This general approach was also used to generate **38**−**39** and **42**−**45** employing the appropriate fragments. Linker-modified **41** featuring a reversed RHS amide was generated similarly by initial formation of the urea followed by deprotection of the aniline, amide coupling, and final deprotection. Preparation of **46** employed an inverted sequence utilizing intermediate **53**, which was heated in the

Scheme 3[a]

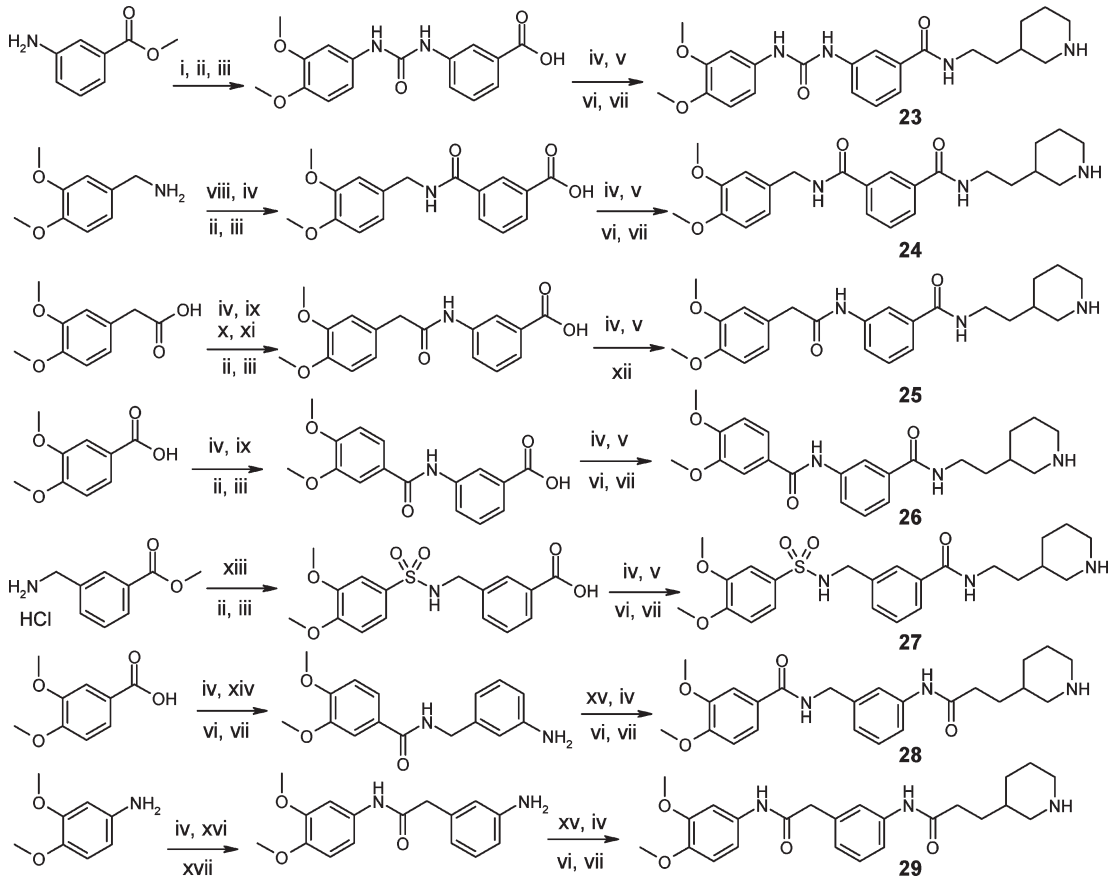

[a] (i) 4-Isocyanato-1,2-dimethoxy-benzene, DMF; (ii) Amberlyst A26 (OH^- form), methanol, DMF, or methanol/DMF; (iii) formic acid, methanol; (iv) *N*-(3-dimethylaminopropyl)-*N*′-ethylcarbodiimide hydrochloride, benzotriazole-1-ol, *N*-methylmorpholine or *N*,*N*-diisopropylethylamine, DMF; (v) 3-(2-amino-ethyl)-piperidine-1-carboxylic acid *tert*-butyl ester (vi) SCX, dichloromethane; (vii) ammonia, methanol; (viii) isophthalic acid monomethyl ester; (ix) 3-aminobenzoic acid methyl ester; (x) SCX; (xi) *Si*-DMA; (xii) HCl, dioxane; (xiii) 3,4-dimethoxy-benzenesulfonyl chloride, *Si*-DMA, DMF; (xiv) 3-(aminomethyl)-1-*N*-boc-aniline; (xv) 3-(2-carboxy-ethyl)-piperidine-1-carboxylic acid *tert*-butyl ester; (xvi) (3-nitrophenyl)-acetic acid; (xvii) ammonium formate, Pd/C, methanol.

Scheme 4[a]

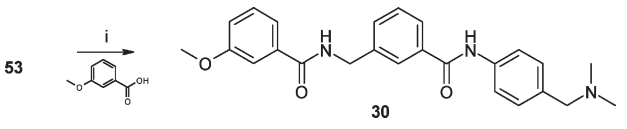

[a] (i) *N*-(3-Dimethylaminopropyl)-*N*′-ethylcarbodiimide hydrochloride, benzotriazole-1-ol, diisopropylethylamine, DMF.

microwave with the preformed symmetrical urea to generate the desired analogue. SCX enabled a catch and release purification. Amides **47**−**50** were acquired by hydrolysis of the corresponding nitriles. Having evaluated several conditions to effect this transformation, we ultimately found sulfuric acid in TFA to be most effective and is exemplified for the synthesis of **47**.

Lead Generation: Selectivity Assessment. We monitored selectivity for the bisbenzamide and ureidobenzamide series during the course of our SAR studies evaluating the potency of selected examples against three of the counterscreening proteins which had shown significant cross-reactivity from the hit set, including PKCε, CDC42BPB, and PKN2. We also tracked ROCK1 activity to confirm that our inhibitors maintained dual potency for the two isoforms. Table 8 shows the selectivity data for representative analogues from both series. The compounds showed similar potency for ROCK isoforms, with most analogues exhibiting a slight preference for ROCK2 including benchmark **1**. Good selectivity for ROCK over the counterscreen panel was observed, with three analogues showing weak and one moderate inhibition of PKN2. However, the degree of cross reactivity for these analogues was not significant as nearly a 100-fold level of selectivity or greater was maintained, and all analogues had improved selectivity as compared to literature benchmarks at the time of our studies.

General kinase selectivity is important for compounds intended for chronic indications, as these proteins are key regulators of cell signaling and homeostasis. As mentioned earlier, the scaffold represented a unique chemotype considering known kinase inhibitors, and we were optimistic that it might provide an opportunity for the development of selective inhibitors. Broad kinase profiling for bisbenzamide **18** (33 nM ROCK2) and urea **50** (4 nM ROCK2) provided evidence to support our optimism. Compound **18** showed no inhibition of an additional 72 kinases tested (IC_{50} > 10 μM or > 50 POC at 3−6 μM) and weak potency for PRKG1 (IC_{50}, 5.6 μM). Urea **50**, inactive against an additional 44 kinases tested (> 50 POC at 3 μM), also afforded modest inhibition of PRKG1 (IC_{50}, 3 μM), and marginal results for PRK2 and PKCα (33 and 50 POC at 3 μM, respectively).

Scheme 5[a]

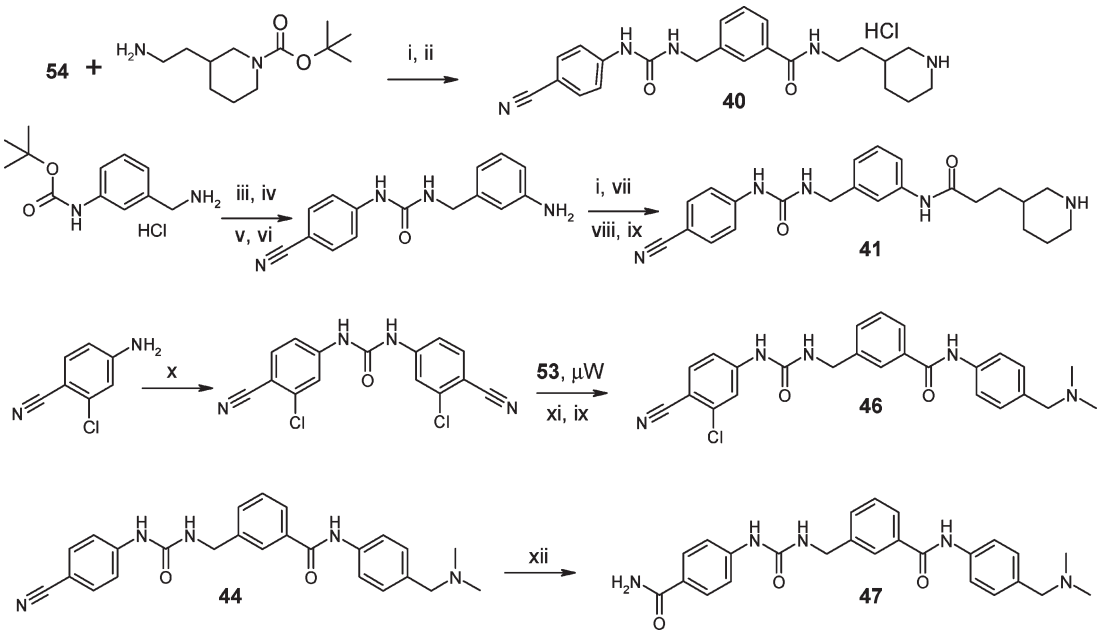

[a] (i) *N*-(3-Dimethylaminopropyl)-*N*′-ethylcarbodiimide hydrochloride, benzotriazole-1-ol, *N*,*N*-diisopropylethylamine or *N*-methylmorpholine, DMF; (ii) HCl, dioxane; (iii) *Si*-DMA, DMF; (iv) *p*-cyanophenylisocyanate, SCX, DMF; (v) SCX; (vi) trifluoroacetic acid, dichloromethane; (vii) 3-(2-carboxy-ethyl)-piperidine-1-carboxylic acid *tert*-butyl ester; DMF; (viii) SCX, dichloromethane; (ix) ammonia, methanol; (x) carbonyldiimidazole, DMF; (xi) SCX, methanol/acetonitrile; (xii) H_2SO_4, trifluoroacetic acid.

Table 8. Selectivity Data for Selected Inhibitors

entry	IC $_{50}$ nM ROCK2	IC_{50} nM ROCK1	IC_{50} nM PKCε	IC_{50} nM CDC42BPB	IC_{50} nM PKN2
15	176	180	> 5000	> 5000	> 5000
17	53	97	> 5000	> 5000	4400
18	33	68	> 5000	> 5000	> 5000
20	46	86	> 5000	> 5000	> 5000
21	69	205	> 5000	> 5000	> 5000
28	73	190	> 5000	> 5000	> 5000
34	92	220	> 5000	> 5000	> 5000
38	89	74	> 5000	> 5000	> 5000
40	18	31	> 5000	> 5000	1700
43	14	40	> 5000	> 5000	1600
44	65	91	> 5000	> 5000	> 5000
50	4	6	> 5000	> 5000	770
1	430	660	3000	> 5,000	780

Again, these values afford > 100-fold selectivity for the additional kinases evaluated (Supporting Information).

Lead Generation: Target Independent Profiling. As mentioned earlier, one of the key challenges associated with the HtL process is the development of ligands identified from biochemical screens into safe and effective pharmacologically active agents. As a response to this challenge, various in vitro profiling tools have been incorporated into the HtL process. For hit compound **5**, we had identified specific issues as a result of this profiling process, which included poor metabolic stability, moderate CYP inhibition (2C9, 3A4), and an apparent efflux problem. As can be seen from the profiling data in Table 9, replacement of the pyridine moiety of **5** with piperidine not only improved the potency but also improved metabolic stability and eliminated CYP inhibition (**15**).[32] However, adding an aromatic into the RHS linker in some cases reestablished variable levels of 3A4 (**20**, **21**, **33**, **43**) and 2C9 (**33**, **43**) activity, but the SAR for CYP inhibition did not correlate to other modifications which improved Rho kinase activity and we therefore felt that this was a manageable problem. However, permeability/efflux remained an issue. We found that passive permeability (PAMPA analysis) could be improved by utilizing a 3° rather than a 2° amine or replacing the amine with an alcohol (**20**, **21**, **22**). But as can be seen in the table, these changes alone did not significantly alter the efflux ratio as determined by Caco-2. An in vivo rat PK study was done on **21** because this analogue showed high permeability in the PAMPA assay. The results revealed very low bioavailability (1.8%) for this compound, apparently resulting from low intestinal absorption possibly due to transport mediated efflux. A potential solution to the unbalanced efflux ratio as measured by Caco-2 was ultimately found when analogues with modifications to the dimethoxy phenyl fragment were evaluated. Replacing the *m*-methoxy moiety with methyl or halogen led to more permeable compounds with a more acceptable B→A/A→B ratio (**33**, **34**). These analogues suffered a modest to moderate loss in potency in the molecular assay, but the modifications provided at least one mechanism to address this lingering issue. The series was also evaluated for hERG activity (**18**), and no inhibition was observed up to 70 μM. These studies helped to define options to improve properties and enabled the series to meet target-independent profiling criteria.

Lead Generation: Functional Analysis. Inhibition of Rho kinase moderates smooth muscle contraction leading to blood vessel relaxation. Our functional assay measured the extent to which our inhibitors could reverse phenylephrine-induced contraction of rat aortic rings.[33] Selected functional results are reported in Table 10. Hit compound **5** demonstrated functional activity equivalent to its molecular potency. Assuming ATP competitive inhibition of Rho kinase is the only enabling mechanism, the absence of a potency shift was unexpected considering the reported $K_{M,ATP}$ for Rho kinase

Table 9. Profiling Data for Rho Kinase Inhibitors

entry	ROCK2 IC_{50} (nM)	sol (μg/mL)[a]	PAMPA $\times$ 10^{-6}	Caco-2[b]	Caco-2[c]	HLM $t_{1/2}$ (m)	CYP 1A2[d]	CYP 2C9[d]	CYP 2C19[d]	CYP 2D6[d]	CYP 3A4[d]
15	176	67	0.6	0.1	0.6	87	> 30[e]	> 30[e]	> 30[e]	> 30[e]	> 30/ > 30[e]
17	53	16	BQL[g]	0.1	0.8	139	> 30[e]	> 30[e]	> 30[e]	> 30[e]	> 30/ > 30[e]
18	33	49	3.6	BQL[g]	5.4	146	> 30[e]	> 30[e]	> 30[e]	> 30[e]	> 30[f]
20	46	> 85	16	0.3	27.1	55	> 30[e]	> 30[e]	> 30[e]	> 30[e]	1.7/ > 30[e]
21	69	> 100	10	BQL[g]	14.6	66	> 30[e]	> 30[e]	> 30[e]	> 30[e]	8.5/ > 30[e]
22	870	48	10	0.6	16.1	41	> 30[f]	> 30[f]	NT[h]	> 30[f]	> 30[f]
43	14	> 100	BQL[g]	BQL[g]	8.8	189	> 30[e]	> 30[e]	22[e]	> 30[e]	5.9/ > 30[e]
33	266	> 88	21	7.9	30.8	NT[h]	> 30[f]	> 30[f]	12.5[f]	> 30[f]	13.5[f]
34	92	> 96	24	7.7	45.3	NT[h]	> 30[f]	> 30[f]	NT[h]	> 30[f]	> 30[f]

[a] HT solubility @ pH 7.4. [b] A to $B \times 10^{-6}$ cm/s. [c] B to $A \times 10^{-6}$ cm/s. [d] μM. [e] Fluorescence assay; 3A4 substrates BFC/BQ. [f] LCMS/MS assay. [g] Below quantifiable limit. [h] Not tested. (See Supporting Information for method details.)

Table 10. Cellular Potency of Selected Inhibitors and Literature Standard **1**

entry	aortic rings IC_{50} (μM)[a]	hROCK2 IC_{50} (nM)	hROCK1 IC_{50} (nM)	shift[b]	PAMPA $\times$ 10^{-6}	Caco-2 ($B \rightarrow A / A \rightarrow B$)
5	1.9	2300	4300	0.82;0.44	NT[c]	29.1/0.5 (58)
18	6.4 ± 3.9	33	68	194;94	3.6	5.4/ < 0.1 (> 54)
20	1.2 ± 0.2	46	70	26;17	16	27.1/0.3 (90.3)
21	6.0 ± 2.8	69	205	87;29	10	14.6/ < 0.1 (> 146)
34	1.6	92	220	17.4;7.3	24	45.3/7.7 (5.9)
43	8.5 ± 2.5	14	40	607;212	BQL[d]	8.8/ < 0.1 (> 88)
1	6.1 ± 1.8	430	660	14.0;9.1	NT[c]	NT[c]

[a] Each individual result is the mean from four different segments from four different rats. Multiple individual results ($n \geq 2$) are reported as the mean ± SEM. [b] Values represent the shift between luciferase molecular data and the aortic ring functional results (ROCK2;ROCK1). [c] Not tested. [d] Below quantifiable limit.

isoforms (1.9 μM ROCK1, 20 μM ROCK2).[34] For the optimized bisbenzamides, we noted an overall average shift of ~40-fold between the ROCK-II molecular and aortic ring functional results. However, the correlation was not always consistent, and we expected that permeability/efflux was at least partially responsible. As can be seen in Table 10, the level of passive permeability as measured by PAMPA in conjunction with the efflux ratios calculated from Caco-2 studies shows a rough correlation to the observed shift. One of our most permeable compounds **34** gave a 17/7-fold (ROCK2/ROCK1) shift similar to the literature benchmark **1**, a significant improvement over related analogue **21**, which had a greater efflux ratio. Likewise, an improvement in passive permeability (PAMPA) for **20** as compared to its demethylated analogue **18** also translated into a smaller shift. Generally, ureidobenzamides demonstrated a greater shift as seen for **43**, and while not as broadly profiled as the bisbenzamide series, permeability/efflux constraints for the ureidobenzamides again appeared to be partially responsible.

Conclusion

In summary, we have identified a bisbenzamide and related ureidobenzamide series of inhibitors of Rho kinase from an HTS discovery approach. The involvement of Rho kinase in various pathological processes renders significance to the development of potent and selective inhibitors as potential drug candidates, as well as agents for evaluating discrete biochemical mechanisms. Our series features a unique kinase platform demonstrating structure-based activity and affording notable selectivity within the kinase gene family (near/ > 100-fold selectivity against all kinases evaluated: 76 results for **18** and 50 results for **50**). A level of selectivity may be accrued as a result of unorthodox binding features in the region we hypothesized to be associated with the hinge, as our SAR studies suggest hydrophobic interactions may predominate. Optimized analogues have shown significant inhibition of the protein, and several have demonstrated moderate potency in our functional assay. We have also identified features of the original hit compound which contributed to poor target-independent properties and have investigated options which improve these deficiencies providing a potential path forward. Overall, these studies supported advancement of the series to lead optimization (LO) whereby further development has led to highly selective, orally bioavailable inhibitors of Rho kinase with potent pharmacological effects. These studies will be reported in due course.

Experimental Section

General Methods. ^{1}H and ^{13}C NMR spectra were recorded on a Bruker UltraShield-400 MHz spectrometer in solvents as noted. Mass spectra were obtained on a Waters ZQ single quadrupole mass spectrometer using electrospray positive/negative ionization. Analytical LC/MS data were recorded on an analytical system consisting of a Waters ZQ mass spectrometer, Agilent 1100 DAD, and Sedex 85 ELS detectors, and an Agilent 1100 HPLC system, equipped with an Eclipse XDB C18 2.5 mm $\times$ 100 mm, 3.5 μm particle diameter, column. A linear gradient from 95% water/acetonitrile (0.1% formic acid) to 95% acetonitrile/water (0.1% formic acid) was used at a flow rate of 2.5 mL/min for 7 min followed by a 2 min hold at 95% acetonitrile/water (0.1% formic acid). Purity for all final compounds (HPLC/MS) is > 95%.

Purification by flash chromatography was accomplished using RediSep prepacked disposable columns run on the Isco Combiflash. Preparative TLC was done using Uniplate silica gel plates purchased from Analtech. Microwave reactions were run in a Smith Synthesizer microwave reactor. Purification by reverse-phase HPLC utilized a mass-directed preparative scale LC/MS FractionLynx system controlled by MassLynx version 3.5. The system consisted of a 2525 high performance liquid chromatography (HPLC) pump, a ZQ single quadrupole mass spectrometer, two 515 high performance liquid chromatography (HPLC) pumps for at column dilution and a makeup pump, a 2767 Sample Manager, and a 2996 photo diode array detector (Waters Corporation, Milford, MA). All samples were purified

on an Atlantis prep dC18 (5 μm particle diameter) 19 mm × 50 mm column. The mobile phases consisted of (A) water with 0.1% formic acid and (B) acetonitrile with 0.1% formic acid. The at column dilution solvent used was methanol with 0.1% formic acid at a constant flow rate of 1 mL/min and an overall system flow rate of 21 mL/min. All solvents were purchased from EM Science. All reagents were purchased from the Aldrich Chemical Co. with the following exceptions: SCX from Varian (Bond Elut SCX) or Silicycle (Silia*Bond* SCX), *Si*-DMA (Silia*Bond* DMA) from Silicycle, *N*-(3-dimethylaminopropyl)-*N*′-ethylcarbodiimide hydrochloride (EDC) from Fluka, 2-pyridin-4-yl-ethylamine from Lancaster, 3-methyl-4-methoxybenzoic acid from Matrix, 4-dimethylaminomethylaniline from J&W Pharma, 4-hydroxymethylaniline from Lancaster, 3-aminomethyl-benzoic acid methyl ester hydrochloride from Maybridge, 3-(2-amino-ethyl)-piperidine-1-carboxylic acid *tert*-butyl ester from Astatech, 3-amino-benzoic acid methyl ester from TCI, 3-chloro-4-trifluoromethoxybenzoic acid from Indofine, 3-(aminomethyl)-1-*N*-boc-aniline from Peakdale, 3-*t*-butoxycarbonylamino-benzyl-ammonium chloride from Peakdale, 3-(2-carboxy-ethyl)-piperidine-1-carboxylic acid *tert*-butyl ester from Astatech, 3-(*tert*-butoxycarbonylamino-methyl)-benzoic acid from Fluka, 3-(3-carboxy-ethyl)-piperidine-1-carboxylic acid *tert*-butyl ester from Astatech, and 7-amino-3,4-dihydro-1H-isoquinoline-2-carboxylic acid *tert*-butyl ester from J&W Pharma. The acronym TFA is used throughout to designate trifluoroacetic acid and DCM to designate dichloromethane. Reported methods are unoptimized.

Standard Coupling Procedure. A carboxylic acid, *N*-(3-dimethylaminopropyl)-*N*′-ethylcarbodiimide hydrochloride (1.1−1.4 equiv), and benzotriazole-1-ol (1.1−1.4 equiv) were combined in a reaction vial and DMF was added (0.1−0.6 mmol acid/mL). The mixture was agitated briefly, and then *N*,*N*-diisopropylethylamine (DIEA) or *N*-methylmorpholine (NMM) (2−3 equiv) was added. The mixture was agitated for 15−30 min, then the amine coupling fragment was added (0.6−1.4 equiv), and the resulting mixture was agitated for 16−70 h. The reaction mixture was diluted with water and extracted with ethyl acetate. The combined extracts were washed with 1N HCl, $NaHCO_3$ (satd aq) and brine (as appropriate to the specific reaction), dried with Na_2SO_4, and concentrated. The isolated amide was either purified or used directly. Alternatively, the reaction mixture was purified directly by preparative HPLC.

Procedures for Synthesis of Common Intermediates 51−54. 3-Aminomethyl-*N*-(2-pyridin-4-yl-ethyl)-benzamide (51). 3-(*tert*-Butoxycarbonylamino-methyl)-benzoic acid (150.7 mg, 0.6 mmol) and 2-pyridin-4-yl-ethylamine (0.06 mL, 0.5 mmol) were coupled using the standard procedure with DIEA. The isolate, [3-(2-pyridin-4-yl-ethylcarbamoyl)-benzyl]-carbamic acid *tert*-butyl ester, which was used without purification, was dissolved in DCM (5 mL) and treated with SCX (1.36 g, 1.2 mmol). The resulting mixture was agitated for 24 h and then filtered. The silica was washed with DCM and methanol. The product was eluted with NH_3 (7 N in methanol), and the eluent was concentrated to provide the title compound (125 mg, 94%). ^{1}H NMR (400 MHz, DMSO-d_6) δ 8.53 (t, J = 7.0 Hz, 1H), 8.49 (dt, J = 4.8, 0.8 Hz, 1H), 7.79 (s, 1H), 7.69 (dt, J = 7.6, 1.8 Hz, 1H), 7.64 (d, J = 7.6 Hz, 1H), 7.47 (d, J = 7.7 Hz, 1H), 7.37 (t, J = 7.6 Hz, 1H), 7.26 (d, J = 7.8 Hz, 1H), 7.20 (ddd, J = 7.5, 3.8, 1.0 Hz, 1H), 3.78 (s, 2H), 3.59 (dt, J = 7.0, 7.0 Hz, 2H), 2.98 (t, J = 7.0 Hz, 2H). ESMS: m/z 256 (M + H). HPLC: 100%.

3-[(3,4-Dimethoxy-benzoylamino)-methyl]-benzoic Acid (52). 3,4-Dimethoxybenzoic acid (400.8 mg, 2.2 mmol) and 3-methoxycarbonyl-benzyl-ammonium chloride (403.3 mg, 2 mmol) were coupled using the standard procedure with DIEA to give 3-[(3,4-dimethoxy-benzoylamino)-methyl]-benzoic acid methyl ester, which was used without purification. The ester was dissolved in a mixture of methanol (6 mL) and DMF (1 mL) and treated with Amberlyst A26 (OH^- form) (3730 mg, 5 mmol), and the resulting mixture was agitated for 36 h. The resin was then filtered and washed with methanol (2 × 4 mL), DMF (1 × 4 mL), and methanol (2 × 4 mL). The product acid was eluted with a solution of 20% formic acid in methanol. The eluent was concentrated, and the resulting solid was triturated in diethylether. The title compound was isolated by filtration (386 mg, 61%). ^{1}H NMR (400 MHz, DMSO-d_6) δ 13.30 (br, 1H) 9.18 (t, J = 5.8 Hz, 1H), 8.47 (s, 1H), 8.13−8.08 (m, 2H), 7.61 (t, J = 7.7 Hz, 1H), 6.96−6.84 (m, 3H), 4.42 (d, J = 5.8 Hz, 2H), 3.74 (s, 3H), 3.72 (s, 3H). ESMS: m/z 316 (M + H). HPLC: 100%.

3-Aminomethyl-*N*-(4-dimethylaminomethyl-phenyl)-benzamide (53). 3-(*tert*-Butoxycarbonylamino-methyl)-benzoic acid (377 mg, 1.5 mmol) and 4-dimethylaminomethylaniline (150 mg, 1 mmol) were coupled using the standard procedure with NMM to provide [3-(4-dimethylaminomethyl-phenylcarbamoyl)-benzyl]-carbamic acid *tert*-butyl ester (265 mg, 69% yield). ESMS: m/z 227 (M + H), which was used without purification. This intermediate was dissolved in DCM (5 mL). and the resulting solution was treated with SCX (2.27 g, 0.88 mmol/g, 2.0 mmol). The mixture was agitated for 16 h. The resin was isolated by filtration and washed with DCM, acetonitrile, and then methanol. The product was eluted with NH_3 (7 N in methanol). The eluent was concentrated to provide the title compound (172 mg, 89.5% yield). ^{1}H NMR (400 MHz, methanol-d_4) δ 7.75 (s, 1H), 7.66 (d, J = 7.8 Hz, 1H), 7.53 (d, J = 8.5 Hz, 2H), 7.41 (d, J = 7.8 Hz, 1H)), 7.32 (t, J = 7.7 Hz, 1H), 7.17 (d, J = 8.5 Hz, 2H), 3.74 (s, 2H), 3.32 (s, 2H), 2.12 (s, 6H). ESMS: m/z 284 (M + H). HPLC: 96%.

3-[3-(4-Cyano-phenyl)-ureidomethyl]-benzoic Acid (54). 3-Methoxycarbonyl-benzyl-ammonium chloride (605 mg, 3.0 mmol) was dissolved in DMF (6 mL) in a reaction vial. *Si*-DMA (3.3 g, 5 mmol) was added, and the mixture was agitated for 1 h. Subsequently, *p*-cyanophenylisocyanate (403.5 mg, 2.8 mmol) was added and the mixture was agitated 16 h. SCX (568 mg, 0.5 mmol) was added, and the mixture was agitated for 30 min. The sorbents were filtered and the filtrate was concentrated to provide 3-[3-(4-cyano-phenyl)-ureidomethyl]-benzoic acid methyl ester (843 mg, 91% yield), which was used directly. The urea was dissolved in THF (7 mL). A solution of lithium hydroxide (410 mg, 10 mmol) in water (3 mL) was added. The resulting mixture was heated at 50 °C for 2 h and then cooled to room temperature. The organic phase was separated, and the remaining aqueous solution was neutralized. The title compound was isolated by filtration (710 mg, 93% yield). ^{1}H NMR (400 MHz, DMSO-d_6) δ 12.98 (s, 1H), 9.21 (s, 1H), 7.90 (s, 1H), 7.83 (d, J = 7.7 Hz, 1H), 7.68 (d, J = 8.8 Hz, 2H), 7.59 (d, J = 8.8 Hz, 2H), 7.55 (d, J = 7.7 Hz, 1H), 7.47 (t, J = 7.7 Hz, 1H), 6.97 (t, J = 6.0 Hz, 1H), 4.37 (d, J = 6.0 Hz, 2H). ESMS: m/z 296 (M + H). HPLC: 92%.

3,4-Dimethoxy-*N*-[3-(2-pyridin-4-yl-ethylcarbamoyl)-benzyl]-benzamide (5). 3,4-Dimethoxybenzoic acid (100 mg, 0.55 mmol) and **51** (100 mg, 0.39 mmol) were coupled using the standard procedure with DIEA. The isolate was purified by flash chromatography using a gradient of ethyl acetate in hexane to provide the title compound (92 mg, 56% yield). ^{1}H NMR (400 MHz, $CDCl_3$) δ 8.42 (d, J = 6.2 Hz, 2H), 7.69 (s, 1H), 7.62 (d, J = 7.7 Hz, 1H), 7.44−7.48 (m, 2H), 7.38−7.28 (m, 4H), 7.18 (t, J = 5.9 Hz, 1H), 7.11 (t, J = 5.9 Hz, 1H), 6.85 (d, J = 8.4 Hz, 1H), 4.58 (d, J = 5.9 Hz, 2H), 3.92 (s, 3H), 3.89 (s, 3H), 3.72 (q, J = 6.3 Hz, 2H), 3.03 (t, J = 6.8 Hz, 2H). ESMS: m/z 420 (M + H).

Using the method described for the synthesis of **5**, compounds **10**−**13** were prepared from the corresponding substituted benzoic acids.

4-Methoxy-*N*-[3-(2-pyridin-4-yl-ethylcarbamoyl)-benzyl]-benzamide (10). Purified by preparative HPLC using an acetonitrile/water/formic acid gradient: 62.9% yield. ^{1}H NMR (400 MHz, $CDCl_3$) δ 8.44 (d, J = 6.2 Hz, 2H), 7.80−7.75 (m, 2H), 7.69 (s, 1H), 7.63 (d, J = 7.7 Hz, 1H), 7.45 (d, J = 7.7 Hz, 1H), 7.40−7.26 (m, 3H), 7.05−6.94 (m, 2H), 6.93−6.88 (m, 2H), 4.58 (d, J = 5.9 Hz, 2H), 3.86 (s, 3H), 3.73 (q, J = 6.7 Hz, 2H), 3.04 (t, J = 6.8 Hz, 2H). ESMS: m/z 390 (M + H).

3-Methoxy-*N*-[3-(2-pyridin-4-yl-ethylcarbamoyl)-benzyl]-benzamide (11). Purified by preparative HPLC using an acetonitrile/water/formic acid gradient: 58% yield. ^{1}H NMR (400 MHz, $CDCl_3$) δ 8.42 (d, J = 6.1 Hz, 2H), 7.69 (s, 1H), 7.62 (d, J = 7.7 Hz, 1H), 7.45 (d, J = 7.7 Hz, 1H), 7.41−7.31 (m, 6H), 7.21 (t, J = 5.9 Hz, 1H), 7.12 (t, J = 5.9 Hz, 1H), 7.08−7.12 (m, 1H), 4.58 (d, J = 5.9 Hz, 2H), 3.82 (s, 3H), 3.72 (q, J = 6.7 Hz, 2H), 3.02 (t, J = 6.8 Hz, 2H). ESMS: m/z 390 (M + H).

1,3-Benzodioxole-5-carboxylic acid 3-(2-pyridin-4-yl-ethylcarbamoyl)-benzylamide (12). Purified by preparative HPLC using an acetonitrile/water/formic acid gradient: 21% yield. ^{1}H NMR (400 MHz, $CDCl_3$) δ 8.55 (d, J = 5.3 Hz, 2H), 7.72 (s, 1H), 7.62 (d, J = 7.6 Hz, 1H), 7.51 (d, J = 7.7 Hz, 1H), 7.43 (t, J = 7.6 Hz, 1H), 7.36−7.23 (m, 4H), 6.85 (d, J = 8.0 Hz, 1H), 6.50 (t, J = 5.9 Hz, 1H), 6.39 (t, J = 5.9 Hz, 1H), 6.06 (s, 2H), 4.66 (d, J = 5.9 Hz, 2H), 3.76 (q, J = 6.7 Hz, 2H), 3.01 (t, J = 6.8 Hz, 2H). ESMS: m/z 404 (M + H).

3,4-Dimethyl-*N*-[3-(2-pyridin-4-yl-ethylcarbamoyl)-benzyl]-benzamide (13). Purified by preparative HPLC using an acetonitrile/water/formic acid gradient: 59.3% yield. ^{1}H NMR (400 MHz, $CDCl_3$) δ 8.43 (d, J = 6.0 Hz, 2H), 7.69 (s, 1H), 7.63 (d, J = 7.7 Hz, 1H), 7.58 (s, 1H), 7.52 (d, J = 7.8 Hz, 1H), 7.44 (d, J = 7.7 Hz, 1H), 7.35 (t, J = 7.7 Hz, 1H), 7.32−7.26 (m, 2H), 7.17 (d, J = 7.9 Hz, 1H), 7.09 (t, J = 5.8 Hz, 1H), 7.03 (t, J = 5.8 Hz, 1H), 4.58 (d, J = 6.0 Hz, 2H), 3.71 (q, J = 6.8 Hz, 2H), 3.01 (t, J = 6.9 Hz, 2H), 2.30 (s, 3H) 2.28 (s, 3H). ESMS: m/z 388 (M + H).

***N*-[3-(Isoquinolin-6-ylcarbamoyl)-benzyl]-3,4-dimethoxy-benzamide (14).** 5-Aminoisoquinoline, (50 mg, 0.35 mmol) and **52** (50 mg, 0.16 mmol) were coupled using the standard procedure with DIEA. The isolate was purified by preparative HPLC using an acetonitrile/water/formic acid gradient to provide the title compound (23 mg, 33% yield). ^{1}H NMR (400 MHz, $CDCl_3$) δ 9.21 (s, 1H), 8.56 (s, 1H), 8.51−8.47 (m, 2H), 7.99 (d, J = 8.9 Hz, 1H), 7.95 (s, 1H), 7.85 (d, J = 7.7 Hz, 1H), 7.74 (dd, J = 8.8, 2.1 Hz, 1H), 7.69 (d, J = 5.9 Hz, 1H), 7.60 (d, J = 8.0 Hz, 1H), 7.57−7.45 (m, 2H), 7.36 (dd, J = 8.4, 2.1 Hz, 1H), 6.88 (d, J = 8.4 Hz, 1H), 6.72 (t, J = 5.9 Hz, 1H), 4.74 (d, J = 6.0 Hz, 2H), 3.95 (s, 3H), 3.94 (s, 3H). ESMS: m/z 442 (M + H).

General Procedure for Synthesis of 15−18. Intermediate **52** and the appropriate amine were coupled using the standard procedure with DIEA. Deprotection was accomplished by dissolution of the amide in DCM (0.1 mmol/mL), followed by treatment with TFA (20% of solvent). The resulting mixture was agitated for 2 h, then concentrated. If needed, purification was done by preparative HPLC using an acetonitrile/water/formic acid gradient or flash chromatography using a methanol DCM gradient.

3,4-Dimethoxy-*N*-[3-(2-piperidin-4-yl-ethylcarbamoyl)-benzyl]-benzamide (15). Purification by flash chromatography using a methanol/DCM gradient provided the title compound, TFA salt: 41% yield. ^{1}H NMR (400 MHz, $CDCl_3$) δ 8.60 (s, br, 1H), 8.27 (s, br, 1H), 7.76 (s, 1H), 7.68 (d, J = 7.6 Hz, 1H), 7.50 (d, J = 7.9 Hz, 1H), 7.43 (t, J = 7.6 Hz, 1H), 7.40−7.32 (m, 2H), 7.12 (t, J = 5.5 Hz, 1H), 6.96 (t, J = 5.5 Hz, 1H), 6.88 (d, J = 8.4 Hz, 1H), 4.67 (d, J = 5.9 Hz, 2H), 3.92 (s, 3H), 3.91 (s, 3H), 3.51−3.38 (m, 4H), 2.88−2.81 (m, 2H), 2.02−1.98 (m, 2H), 1.73−1.46 (m, 5H). ESMS: m/z 426 (M + H).

3,4-Dimethoxy-*N*-[3-(1,2,3,4-tetrahydro-isoquinolin-6-ylcarbamoyl)-benzyl]-benzamide (16). Purification by preparative HPLC using an acetonitrile/water/formic acid gradient provided the title compound: 35% yield. ^{1}H NMR (400 MHz, methanol-d_4) δ 7.81 (s, 1H), 7.70 (d, J = 8.7 Hz, 1H), 7.49−7.32 (m, 6H), 6.93−6.90 (m, 2H), 4.54 (s, 2H), 3.86 (s, 2H), 3.78 (s, 3H), 3.77 (s, 3H), 3.00 (t, J = 6.0 Hz, 2H), 2.75 (t, J = 6.0 Hz, 2H). ESMS: m/z 446 (M + H).

3,4-Dimethoxy-*N*-[3-(2-piperidin-3-yl-ethylcarbamoyl)-benzyl]-benzamide (17). TFA salt: 74% yield. ^{1}H NMR (400 MHz, $CDCl_3$) δ 8.81 (s, br, 1H), 8.58 (s, br, 1H), 7.86 (t, J = 5.5 Hz, 1H), 7.68 (s, 1H), 7.63−7.55 (m, 2H), 7.48−7.36 (m, 3H), 7.34−7.28 (m, 1H), 6.84 (d, J = 8.3 Hz, 1H), 4.54 (d, J = 5.0 Hz, 2H), 3.89 (s, 3H), 3.84 (s, 3H), 3.51−3.21 (m, 4H), 2.86−2.68 (m, 1H), 2.55−2.37 (m, 1H), 1.96−1.63 (m, 4H), 1.63−1.37 (m, 2H), 1.22−1.01 (m, 1H). ESMS: m/z 426 (M + H).

3,4-Dimethoxy-*N*-[3-(1,2,3,4-tetrahydro-isoquinolin-7-ylcarbamoyl)-benzyl]-benzamide (18). Purification by preparative HPLC using an acetonitrile/water/formic acid gradient provided the title compound: 25% yield. ^{1}H NMR (400 MHz, DMSO-d_6) δ 10.22 (s, 1H), 9.01 (t, J = 6.0 Hz, 1H), 7.89 (s, 1H), 7.83 (d, J = 13.3 Hz, 1H), 7.61−7.41 (m, 6H), 7.11 (d, J = 8.4 Hz, 1H), 7.04 (d, J = 8.5 Hz, 1H), 4.55 (d, J = 5.9 Hz, 2H), 4.20 (s, 2H), 3.82 (s, 3H), 3.81 (s, 3H), 3.13 (t, J = 5.9 Hz, 2H), 2.79 (t, J = 5.8 Hz, 2H). ESMS: m/z 446 (M + H).

3,4-Dimethoxy-*N*-{3-[2-(1-methyl-piperidin-3-yl)-ethylcarbamoyl]-benzyl}-benzamide (19). Compound **17** (80 mg, 0.188 mmol) was dissolved in formic acid (0.5 mL) and formaldehyde (0.5 mL, 37% aqueous solution) was added. The resulting mixture was heated at 70 °C 16 h. The reaction mixture was concentrated, and the isolate was purified by preparative HPLC using an acetonitrile/water/formic acid gradient providing the title compound (41 mg, 50% yield). ^{1}H NMR (400 MHz, DMSO-d_6) δ 8.97 (t, J = 5.9 Hz, 1H), 8.46 (t, J = 5.5 Hz, 1H), 7.79 (s, 1H), 7.70 (d, J = 7.4 Hz, 1H), 7.54 (dd, J = 8.4, 2.0 Hz, 1H), 7.49 (d, J = 1.9 Hz, 1H), 7.47−7.38 (m, 2H), 7.04 (d, J = 8.5 Hz, 1H), 4.51 (d, J = 5.8 Hz, 2H), 3.81 (s, 3H), 3.80 (s, 3H), 3.28 (dd, J = 12.9, 6.9 Hz, 4H), 2.92−2.76 (m, 2H), 2.28 (s, 3H), 2.13−1.99 (m, 1H), 1.91−1.69 (m, 2H), 1.68−1.55 (m, 1H), 1.56−1.34 (m, 2H), 0.88 (dd, J = 22.8, 11.1 Hz, 1H). ESMS: m/z 440 (M + H).

3,4-Dimethoxy-*N*-[3-(2-methyl-1,2,3,4-tetrahydro-isoquinolin-7-ylcarbamoyl)-benzyl]-benzamide (20). Prepared from **18** according to the procedure described for the synthesis of **19**: 22% yield. ^{1}H NMR (400 MHz, $CDCl_3$) δ 9.15 (s, 1H), 7.87 (s, 1H), 7.77 (d, J = 7.7 Hz, 1H), 7.65 (s, 1H), 7.52−7.33 (m, 6H), 7.03 (d, J = 8.3 Hz, 1H), 6.81 (d, J = 8.4 Hz, 1H), 4.59 (d, J = 5.5 Hz, 2H), 3.98 (s, br, 2H), 3.88 (s, 3H), 3.85 (s, 3H), 3.32 (s, br, 2H), 3.05 (s, br, 2H), 2.78 (s, 3H). ESMS: m/z 460 (M + H).

***N*-[3-(4-Dimethylaminomethyl-phenylcarbamoyl)-benzyl]-3,4-dimethoxy-benzamide (21).** 4-Dimethylaminomethylaniline (25.5 mg, 0.17 mmol) and **52** (40 mg, 0.13 mmol) were coupled using the standard procedure with NMM. Purification by preparative HPLC using an acetonitrile/water/formic acid gradient provided the title compound (37 mg, 65% yield). ^{1}H NMR (400 MHz, DMSO-d_6) δ 10.24 (s, 1H), 9.00 (t, J = 5.9 Hz, 1H), 7.89 (s, 1H), 7.84 (d, J = 7.3 Hz, 1H), 7.71 (d, J = 8.4 Hz, 2H), 7.61−7.43 (m, 4H), 7.29 (d, J = 8.4 Hz, 2H), 7.04 (d, J = 8.4 Hz, 1H), 4.56 (d, J = 5.9 Hz, 2H), 3.85 (s, 3H), 3.84 (s, 3H), 3.42 (s, 2H), 2.18 (s, 6H). ESMS: m/z 448 (M + H).

***N*-[3-(4-Hydroxymethyl-phenylcarbamoyl)-benzyl]-3,4-dimethoxy-benzamide (22).** 4-Hydroxyomethylaniline (19.7 mg, 0.16 mmol) and **52** (45.0 mg, 0.14 mmol) were coupled using the standard procedure with NMM purification by preparative HPLC using an acetonitrile/water/formic acid gradient provided the title compound (41 mg, 68% yield). ^{1}H NMR (400 MHz, DMSO-d_6) δ 10.27 (s, 1H), 9.00 (t, J = 5.9 Hz, 1H), 7.89 (s, 1H), 7.83 (d, J = 7.3 Hz, 1H), 7.72 (d, J = 8.3 Hz, 2H), 7.56−7.47 (m, 4H), 7.27 (d, J = 8.4 Hz, 2H), 7.04 (d, J = 8.4 Hz, 1H), 5.14 (t, J = 5.7 Hz, 1H), 4.56 (d, J = 5.9 Hz, 2H), 4.46 (d, J = 5.9 Hz, 2H), 3.85 (s, 3H), 3.84 (s, 3H). ESMS: m/z 419 (M − H).

3-[3-(3,4-Dimethoxy-phenyl)-ureido]-*N*-(2-piperidin-3-yl-ethyl)-benzamide (23). 3-Amino-benzoic acid methyl ester (75.6 mg, 0.5 mmol) was dissolved in DMF (2 mL) in a reaction vial, and 4-isocyanato-1,2-dimethoxy-benzene (98.5 mg, 0.55 mmol) was added. The reaction mixture was agitated 7 h, diluted with DMF (1 mL), and treated with Amberlyst A26 (OH^- form) (1.12 g, 1.5 mmol). The resulting mixture was agitated at ambient temperature for 16 h. The sorbent was filtered and washed with several portions of methanol. The product was eluted with 20% formic acid in methanol, and the sorbent was then washed with several portions of DMF. The eluent was concentrated to a solid which was triturated in methanol. Filtration provided 3-[3-(3,4-dimethoxy-phenyl)-ureido]-benzoic acid (106 mg, 67% yield).

^{1}H NMR (400 MHz, DMSO-d_6) δ 12.93 (s, 1H), 8.80 (s, 1H), 8.53 (s, 1H), 8.14 (s, 1H), 7.61 (d, J = 8.0 Hz, 1H), 7.54 (d, J = 7.8 Hz, 1H), 7.39 (t, J = 7.9 Hz, 1H), 7.23 (s, 1H), 6.88 (s, 2H), 3.75 (s, 3H), 3.71 (s, 3H). ESMS: m/z 317 (M + H). HPLC: 95%. This intermediate (47.4 mg, 0.15 mmol) and 3-(2-amino-ethyl)-piperidine-1-carboxylic acid *tert*-butyl ester (34.3 mg, 0.16 mmol) were coupled using the standard procedure with NMM. The isolate was dissolved directly in DCM (1 mL) and treated with SCX (398 mg, 0.35 mmol), and the resulting mixture was agitated for 16 h. The mixture was filtered and the sorbent was washed with several portions of DCM and methanol. The product was eluted with NH_3 (7N in methanol). The eluent was concentrated providing the title compound (53 mg, 82.8% yield). ^{1}H NMR (400 MHz, DMSO-d_6) δ 8.81 (s, 1H), 8.62 (s, 1H), 8.39 (t, J = 5.5 Hz, 1H), 7.87 (s, 1H), 7.59 (d, J = 7.9 Hz, 1H), 7.40 (d, J = 7.8 Hz, 1H), 7.33 (t, J = 7.8 Hz, 1H), 7.23 (s, 1H), 6.87 (s, 2H), 3.74 (s, 3H), 3.71 (s, 3H), 3.31−3.20 (m, 2H), 2.96 (d, J = 11.2 Hz, 1H), 2.87 (d, J = 12.0 Hz, 1H), 2.45−2.38 (m, 1H), 2.24−2.08 (m, 1H), 1.80 (d, J = 14.8 Hz, 1H), 1.59−1.52 (m, 1H), 1.47−1.31 (m, 4H), 1.08−0.94 (m, 1H). ESMS: m/z 427 (M + H).

***N*-(3,4-Dimethoxy-benzyl)-*N*-(2-piperidin-3-yl-ethyl)-isophthalamide (24).** Isophthalic acid monomethyl ester (180.2 mg, 1.0 mmol) and 3,4-dimethoxybenzylamine (0.167 mL, 1.1 mmol) were coupled using the standard procedure with NMM to provide *N*-(3,4-dimethoxy-benzyl)-isophthalamic acid methyl ester (350 mg, 98% yield). ESMS: m/z 330 (M + H). HPLC: 95%, which was used directly. This intermediate was dissolved in methanol/DMF (4/1, 5 mL) and treated with Amberlyst A26 (OH^- form) (1.9 g, 2.5 mmol). The resulting mixture was agitated at ambient temperature for 36 h. The sorbent was filtered and washed with several protions of methanol and DMF. The product was eluted with 20% formic acid in methanol, and the sorbent was then washed with methanol and DMF. The eluent was concentrated to *N*-(3,4-dimethoxy-benzyl)-isophthalamic acid (240 mg, 76% yield). ^{1}H NMR (400 MHz, DMSO-d_6) δ 12.96 (br, 1H), 9.00 (t, J = 5.9 Hz, 1H), 7.96 (s, 1H), 7.83 (d, J = 7.5 Hz, 1H), 7.58−7.44 (m, 4H), 7.04 (d, J = 8.4 Hz, 1H), 4.53 (d, J = 5.9 Hz, 2H), 3.81 (s, 3H), 3.80 (s, 3H). ESMS: m/z 316 (M + H). HPLC: 100%. This intermediate (44.1 mg, 0.14 mmol) and 3-(2-amino-ethyl)-piperidine-1-carboxylic acid *tert*-butyl ester (34.3 mg, 0.16 mmol) were coupled using the standard procedure with NMM. The isolate was dissolved directly in DCM (1 mL) and treated with SCX (398 mg, 0.35 mmol), and the resulting mixture was agitated for 16 h. The mixture was filtered and the sorbent was washed with several portions of DCM and methanol. The product was eluted with NH_3 (7N in methanol). The eluent was concentrated to the title compound (48 mg, 59.6% yield). ^{1}H NMR (400 MHz, DMSO-d_6) δ 9.08 (t, J = 5.8 Hz, 1H), 8.56 (t, J = 5.5 Hz, 1H), 8.33 (s, 1H), 8.05−7.90 (m, 2H), 7.56 (t, J = 7.7 Hz, 1H), 6.97 (d, J = 1.5 Hz, 1H), 6.94−6.83 (m, 2H), 4.42 (d, J = 5.8 Hz, 2H), 3.74 (s, 3H), 3.72 (s, 3H), 3.33−3.23 (m, 2H), 2.95 (d, J = 11.9 Hz, 1H), 2.86 (d, J = 11.8 Hz, 1H), 2.49−2.36 (m, 1H), 2.24−2.12 (m, 1H), 1.80 (d, J = 13.9 Hz, 1H), 1.59−1.50 (m, 1H), 1.51−1.30 (m, 4H), 1.09−0.93 (m, 1H). ESMS: m/z 426 (M + H).

3-[2-(3,4-Dimethoxy-phenyl)-acetylamino]-*N*-(2-piperidin-3-yl-ethyl)-benzamide (25). (3,4-Dimethoxy-phenyl)-acetic acid (215.8 mg, 1.1 mmol) was dissolved in DMF (7 mL). *N*-(3-dimethylamino-propyl)-*N*′-ethylcarbodiimide hydrochloride (249 mg, 1.3 mmol) and benzotriazole-1-ol (175.7 mg, 1.3 mmol) were added, followed by DIEA (0.23 mL, 1.32 mmol). The resulting mixture was agitated for 1 h, and 3-aminobenzoic acid methyl ester (151.2 mg, 1.0 mmol) was added. The reaction mixture was agitated for 16 h, then treated with SCX (1.7 g, 1.5 mmol) and *Si*-DMA (1.33 g, 2.0 mmol) and the resulting mixture was agitated for 2 h and then filtered. The filtrate was concentrated to 3-[2-(3,4-dimethoxy-phenyl)-acetylamino]-benzoic acid methyl ester. ESMS: m/z 330 (M + H). HPLC: 100%, which was used directly. This intermediate was dissolved in methanol (5 mL) and treated with Amberlyst A26 (OH^- form) (1.5 g, 2 mmol). The resulting mixture was agitated at ambient temperature for 72 h. The sorbent was filtered and washed with several portions of methanol and DMF. The product was eluted with 20% formic acid in methanol and the sorbent was then washed with methanol and DMF. The eluent was concentrated to 3-[2-(3,4-dimethoxy-phenyl)-acetylamino]-benzoic acid (137 mg, 43% yield). ^{1}H NMR (400 MHz, DMSO-d_6) δ 13.00 (br, 1H), 10.30 (s, 1H), 8.23 (s, 1H), 7.81 (d, J = 8.0 Hz, 1H), 7.61 (d, J = 7.8 Hz, 1H), 7.42 (t, J = 7.8 Hz, 1H), 6.96 (s, 1H), 6.91−6.84 (m, 2H), 3.75 (s, 3H), 3.72 (s, 3H), 3.57 (s, 2H). ESMS: m/z 316 (M + H). HPLC: 100%. This intermediate (37.8 mg, 0.12 mmol) and 3-(2-amino-ethyl)-piperidine-1-carboxylic acid *tert*-butyl ester (32 mg, 0.14 mmol) were coupled using the standard procedure with DIEA. The reaction mixture was purified directly by preparative HPLC using an acetonitrile/water/formic acid gradient to provide 3-(2-{3-[2-(3,4-dimethoxy-phenyl)-acetylamino]-benzoyl-amino}-ethyl)-piperidine-1-carboxylic acid *tert*-butyl ester (53 mg, 84% yield). ESMS: m/z 526 (M + H). HPLC: 100%. This intermediate (53 mg, 0.1 mmol) was taken up in 0.5 M HCl in dioxane (1 mL) and methanol (0.5 mL). The mixture was agitated for 1 h then concentrated. The isolate was purified by preparative HPLC using an acetonitrile/water/formic acid gradient to provide the title compound (19 mg, 45% yield). ^{1}H NMR (400 MHz, DMSO-d_6) δ 10.39 (s, 1H), 8.47 (t, J = 5.5 Hz, 1H), 8.04 (s, 1H), 7.78 (d, J = 9.2 Hz, 1H), 7.48 (d, J = 7.8 Hz, 1H), 7.37 (t, J = 7.9 Hz, 1H), 6.97 (s, 1H), 6.95−6.78 (m, 2H), 3.75 (s, 3H), 3.72 (s, 3H), 3.56 (s, 2H), 3.27 (dd, J = 12.8, 6.7 Hz, 2H), 3.16 (d, J = 11.9 Hz, 1H), 3.09 (d, J = 12.4 Hz, 1H), 2.64 (t, J = 12.2 Hz, 1H), 2.47−2.34 (m, 1H), 1.83 (d, J = 10.9 Hz, 1H), 1.77−1.64 (m, 1H), 1.55−1.35 (m, 4H), 1.18−1.01 (m, 1H). ESMS: m/z 426 (M + H).

3,4-Dimethoxy-*N*-[3-(2-piperidin-3-yl-ethylcarbamoyl)-phenyl]-benzamide (26). 3,4-Dimethoxybenzoic acid (364.3 mg, 2.0 mmol) and 3-aminobenzoic acid methyl ester (302.3 mg, 2.0 mmol) were coupled using the standard procedure with NMM to provide 3-(3,4-dimethoxy-benzoylamino)-benzoic acid methyl ester: ESMS: m/z 316 (M + H). HPLC: 95%, which was used directly. This intermediate was dissolved in DMF (3 mL) and treated with Amberlyst A26 (OH^- form) (3.0 g, 4.0 mmol). The resulting mixture was agitated at ambient temperature for 16 h. The sorbent was filtered and washed with several portions of methanol. The product was eluted with 20% formic acid in methanol, and the sorbent was then washed with methanol. The eluent was concentrated to 3-(3,4-dimethoxy-benzoylamino)-benzoic acid (130 mg, 22% yield). ESMS: m/z 302 (M + H). HPLC: 85%. This intermediate (44 mg, 0.15 mmol) and 3-(2-amino-ethyl)-piperidine-1-carboxylic acid *tert*-butyl ester (36.5 mg, 0.16 mmol) were coupled using the standard procedure with NMM. The reaction mixture was purified directly by preparative HPLC using an acetonitrile/water/formic acid gradient to provide 3-{2-[3-(3,4-dimethoxy-benzoylamino)-benzoylamino]-ethyl}-piperidine-1-carboxylic acid *tert*-butyl ester (48 mg, 64.2% yield). ESMS: m/z 512 (M + H). HPLC: 100%. This intermediate (48 mg, 0.094 mmol) was dissolved in DCM (1 mL) and treated with SCX (200 mg, 0.175 mmol), and the resulting mixture was agitated for 16 h. The mixture was filtered, and the sorbent was washed with several portions of DCM and methanol. The product was eluted with NH_3 (7N in methanol). The eluent was concentrated then taken up in 1N HCl aq (1 mL) and methanol (1 mL). The mixture was agitated briefly and then concentrated to provide the title compound, HCl salt (29 mg, 72.5% yield). ^{1}H NMR (400 MHz, DMSO-d_6) δ 10.21 (s, 1H), 9.03 (br, 1H), 8.72 (br, 1H), 8.53 (t, J = 5.9 Hz, 1H), 8.22 (s, 1H), 7.96 (d, J = 7.9 Hz, 1H), 7.68 (d, J = 8.4 Hz, 1H), 7.60−7.52 (m, 2H), 7.42 (t, J = 7.9 Hz, 1H), 7.10 (d, J = 8.5 Hz, 1H), 3.85 (s, 3H), 3.85 (s, 3H), 3.40−3.12 (m, 4H), 2.80−2.68 (m, 1H), 2.60−2.48 (m, 1H), 1.92−1.72 (m, 3H), 1.70−1.40 (m, 3H), 1.22−1.08 (m, 1H). ESMS: m/z 412 (M + H).

3-[(3,4-Dimethoxy-benzenesulfonylamino)-methyl]-*N*-(2-piperidin-3-yl-ethyl)-benzamide (27). 3-Aminomethyl-benzoic acid methyl ester, hydrochloride (201.6 mg, 1.0 mmol) was dissolved in DMF (3 mL) and *Si*-DMA (2.0 g, 3.0 mmol) was added, and the resulting mixture was agitated for 30 min, after which time, 3,4-dimethoxybenzenesulfonyl chloride (236.7 mg, 1.0 mmol) was added and the reaction mixture was agitated for 16 h. The sorbent was filtered and washed with DMF, and the filtrate was concentrated. The isolate was dissolved in DCM (10 mL) and the solution was washed with 1N HCl (5 mL) and brine (5 mL), dried with Na_2SO_4, and concentrated to 3-[(3,4-dimethoxy-benzenesulfonylamino)-methyl]-benzoic acid methyl ester. ESMS: m/z 366 (M + H). HPLC: 100%, which was used directly. This intermediate was dissolved in methanol/DMF (1:1, 3 mL) and treated with Amberlyst A26 (OH^- form) (1.5 g, 2.0 mmol). The resulting mixture was agitated at ambient temperature for 16 h. The sorbent was filtered and washed with several portions of methanol. The product was eluted with 20% formic acid in methanol. The eluent was concentrated to 3-[(3,4-dimethoxy-benzenesulfonylamino)-methyl]-benzoic acid (192 mg, 54.6% yield). ^{1}H NMR (400 MHz, DMSO-d_6) δ 12.95 (br, 1H), 8.09 (t, J = 6.4 Hz, 1H), 7.82 (s, 1H), 7.78 (d, J = 7.7 Hz, 1H), 7.47 (d, J = 7.7 Hz, 1H), 7.41−7.34 (m, 2H), 7.25 (d, J = 2.1 Hz, 1H), 7.07 (d, J = 8.5 Hz, 1H), 4.03 (d, J = 6.4 Hz, 2H), 3.82 (s, 3H), 3.78 (s, 3H). ESMS: m/z 352 (M + H). HPLC: 100%. This intermediate (49.2 mg, 0.14 mmol) and 3-(2-amino-ethyl)-piperidine-1-carboxylic acid *tert*-butyl ester (34.3 mg, 0.15 mmol) were coupled using the standard procedure with NMM. The reaction mixture purified directly by preparative HPLC using an acetonitrile/water/formic acid gradient to provide 3-(2-{3-[(3,4-dimethoxy-benzenesulfonylamino)-methyl]-benzoylamino}-ethyl)-piperidine-1-carboxylic acid *tert*-butyl ester (53 mg, 67.4% yield). ESMS: m/z 562 (M + H). HPLC: 100%. This intermediate (53 mg, 0.094 mmol) was dissolved in DCM (1 mL) and treated with SCX (200 mg, 0.175 mmol), and the resulting mixture was agitated for 16 h. The mixture was filtered and the sorbent was washed with several portions of DCM and methanol. The product was eluted with NH_3 (7N in methanol). The eluent was concentrated then taken up in 1 M HCl aq (1 mL) and methanol (1 mL). The mixture was agitated briefly and then concentrated to provide the title compound, HCl salt (30 mg, 68.9% yield). ^{1}H NMR (400 MHz, DMSO-d_6) δ 9.05 (br, 1H), 8.72 (br, 1H), 8.52 (t, J = 5.5 Hz, 1H), 8.09 (t, J = 5.8 Hz, 1H), 7.77 (s, 1H), 7.71 (d, J = 7.0 Hz, 1H), 7.44−7.28 (m, 4H), 7.10 (d, J = 8.5 Hz, 1H), 3.97 (d, J = 5.6 Hz, 2H), 3.83 (s, 3H), 3.78 (s, 3H), 3.42−3.12 (m, 4H), 2.80−2.62 (m, 1H), 2.58−2.43 (m, 1H), 1.92−1.70 (m, 3H), 1.70−1.38 (m, 3H), 1.21−1.08 (m, 1H). ESMS: m/z 462 (M + H).

3,4-Dimethoxy-*N*-[3-(3-piperidin-3-yl-propionylamino)-benzyl]-benzamide (28). 3,4-Dimethoxybenzoic acid (100 mg, 0.55 mmol) and 3-(aminomethyl)-1-*N*-boc-aniline (111 mg, 0.5 mmol) were coupled using the standard procedure with NMM to provide {3-[(3,4-dimethoxy-benzoylamino)-methyl]-phenyl}-carbamic acid *tert*-butyl ester (190 mg, 89% yield). This intermediate was dissolved in DCM (2 mL). SCX (1.14 g, 1.0 mmol) was added to the solution, and the resulting mixture was agitated for 48 h. The reaction mixture was filtered and the sorbent was washed with DCM (2 × 2 mL) and methanol (2 × 2 mL). The product was eluted with NH_3 (7N in methanol). The eluent was concentrated to provide *N*-(3-amino-benzyl)-3,4-dimethoxy-benzamide (112 mg, 78% yield). ESMS: m/z 287 (M + H). HPLC: 100%. 3-(2-Carboxy-ethyl)-piperidine-1-carboxylic acid *tert*-butyl ester (41.2 mg, 0.16 mmol) and the intermediate prepared above, *N*-(3-amino-benzyl)-3,4-dimethoxy-benzamide (45.8 mg, 0.16 mmol), were coupled using the standard procedure with NMM to provide 3-(2-{3-[(3,4-dimethoxy-benzoylamino)-methyl]-phenylcarbamoyl}-ethyl)-piperidine-1-carboxylic acid *tert*-butyl ester (84 mg, 100% yield). ESMS: m/z 526 (M + H). HPLC: 100%. This intermediate (84 mg 0.16 mmol) was dissolved directly in DCM (1 mL) and treated with SCX (400 mg, 0.35 mmol). The resulting mixture was agitated 16 h. The reaction mixture was filtered, and the solids were washed with DCM (2 × 2 mL) and methanol (2 × 2 mL). The product was eluted with NH_3 (7N in methanol), and the eluent was concentrated to provide the title compound (24 mg, 35% yield). ^{1}H NMR (400 MHz, DMSO-d_6) δ 9.87 (s, 1H), 8.92 (t, J = 5.9 Hz, 1H), 7.57−7.48 (m, 4H), 7.23 (t, J = 7.8 Hz, 1H), 7.03 (d, J = 8.5 Hz, 1H), 6.98 (d, J = 7.6 Hz, 1H), 4.43 (d, J = 5.9 Hz, 2H), 3.81 (s, 3H), 3.80 (s, 3H), 2.92 (d, J = 11.3 Hz, 1H), 2.85 (d, J = 11.8 Hz, 1H), 2.39 (td, J = 11.8, 2.7 Hz, 1H), 2.28 (t, J = 7.6 Hz, 2H), 2.18−2.08 (m, 1H), 1.75 (d, J = 13.8 Hz, 1H), 1.60−1.21 (m, 5H), 1.04−0.93 (m, 1H). ESMS: m/z 426 (M + H).

***N*-{3-[(3,4-Dimethoxy-phenylcarbamoyl)-methyl]-phenyl}-3-piperidin-3-yl-propionamide (29).** 3-Nitrophenylacetic acid (136 mg, 0.75 mmol) and 3,4-dimethoxyaniline (115 mg, 0.75 mmol) were coupled using the standard procedure with NMM. The isolate was purified by preparative HPLC using an acetonitrile/water/formic acid gradient to provide *N*-(3,4-dimethoxy-phenyl)-2-(3-nitro-phenyl)-acetamide (36 mg, 15% yield). This intermediate (36 mg, 0.114 mmol) was dissolved in methanol (1 mL) and ammonium formate (69 mg, 1.1 mmol) then Pd/C (5 mg) were added. The reaction vial was sealed and agitated at 45 °C 16 h. The reaction mixture was filtered, and the filtrate was diluted with ethyl acetate (10 mL). This mixture was washed with water (2 × 5 mL) and brine (1 × 5 mL), dried with Na_2SO_4, and concentrated to provide the intermediate 2-(3-amino-phenyl)-*N*-(3,4-dimethoxy-phenyl)-acetamide (10 mg, 31% yield). ESMS: m/z 287 (M + H). HPLC: 95%. 3-(2-Carboxy-ethyl)-piperidine-1-carboxylic acid *tert*-butyl ester (12.9 mg, 0.05 mmol) and the intermediate prepared above (10 mg, 0.035 mmol) were coupled using the standard procedure with NMM to provide 3-(2-{3-[(3,4-dimethoxy-phenylcarbamoyl)-methyl]-phenylcarbamoyl}-ethyl)-piperidine-1-carboxylic acid *tert*-butyl ester (19 mg, 72% yield). This intermediate was dissolved directly in DCM (1 mL) and treated with SCX (136 mg, 0.12 mmol). The resulting mixture was agitated 16 h, filtered, and the sorbent was washed with DCM (2 × 2 mL) and methanol (2 × 2 mL). The product was eluted with NH_3 (7N in methanol), and the eluent was concentrated. The isolate was purified by preparative HPLC using an acetonitrile/water/formic acid gradient providing the title compound (6.5 mg, 38% yield). ^{1}H NMR (400 MHz, methanol-d_4) δ 7.57 (s, 1H), 7.46 (d, J = 8.1 Hz, 1H), 7.35−7.22 (m, 2H), 7.09 (d, J = 7.6 Hz, 1H), 7.02 (dd, J = 8.6, 2.4 Hz, 1H), 6.87 (d, J = 8.7 Hz, 1H), 3.79 (s, 3H), 3.78 (s, 3H), 3.63 (s, 2H), 3.39−3.26 (m, 2H), 2.87 (td, J = 12.8, 3.1 Hz, 1H), 2.65 (t, J = 12.0 Hz, 1H), 2.49−2.37 (m, 2H), 1.95 (t, J = 16.3 Hz, 2H), 1.85−1.53 (m, 4H), 1.32−1.15 (m, 1H). ESMS: m/z 426 (M + H).

***N*-[3-(4-Dimethylaminomethyl-phenylcarbamoyl)-benzyl]-3-methoxy-benzamide (30).** 3-Methoxybenzoic acid (40 mg, 0.26 mmol) and **53** (40 mg, 0.14 mmol) were coupled using the standard procedure with DIEA. The isolate was purified by preparative HPLC using an acetonitrile/water/formic acid gradient providing the title compound (16 mg, 27% yield). ^{1}H NMR (400 MHz, $CDCl_3$) δ 8.75 (s, 1H), 7.91 (s, 1H), 7.83 (d, J = 9.0 Hz, 1H), 7.74 (d, J = 8.6 Hz, 2H), 7.57 (d, J = 7.8 Hz, 1H), 7.47 (d, J = 7.7 Hz, 1H), 7.46−7.42 (m, 1H), 7.41−7.30 (m, 4H), 7.06 (ddd, J = 7.6, 2.6, 1.6 Hz, 1H), 7.01 (t, J = 5.8 Hz, 1H), 4.70 (d, J = 5.9 Hz, 2H), 3.92 (s, 2H), 3.85 (s, 3H), 2.55 (s, 6H). ESMS: m/z 418 (M + H).

Compounds **31**−**37** were prepared from **53** and the corresponding substituted benzoic acid according to the procedure described for the synthesis of **30**.

***N*-[3-(4-Dimethylaminomethyl-phenylcarbamoyl)-benzyl]-4-methoxy-benzamide (31).** Yield 14%. ^{1}H NMR (400 MHz, $CDCl_3$) δ 8.82 (br, 1H), 7.90 (s, 1H), 7.82 (d, J = 8.8 Hz, 3H), 7.75 (d, J = 8.4 Hz, 2H), 7.56 (d, J = 7.2 Hz, 1H), 7.47 (d, J = 7.6 Hz, 1H), 7.38 (d, J = 8.0 Hz, 2H), 6.93 (d, J = 8.7 Hz, 3H), 4.69 (d, J = 5.8 Hz, 2H), 3.96 (s, 2H), 3.86 (s, 3H), 2.57 (s, 6H). ESMS: m/z 418 (M + H).

***N*-[3-(4-Dimethylaminomethyl-phenylcarbamoyl)-benzyl]-3,4-dihydroxy-benzamide (32).** Yield 10%. ^{1}H NMR (400 MHz, methanol-d_4) δ 7.93 (s, 1H), 7.90−7.82 (m, 3H), 7.61 (d, J = 7.7 Hz, 1H), 7.55−7.47 (m, 3H), 7.35 (d, J = 2.2 Hz, 1H), 7.29 (dd, J = 8.3, 2.2 Hz, 1H), 6.83 (d, J = 8.3 Hz, 1H), 4.64 (s, 2H), 4.28 (s, 2H), 2.86 (s, 6H). ESMS: m/z 420 (M + H).

***N*-[3-(4-Dimethylaminomethyl-phenylcarbamoyl)-benzyl]-4-methoxy-3-methyl-benzamide (33).** Yield 29%. ^{1}H NMR (400 MHz, $CDCl_3$) δ 8.80 (s, 1H), 7.63 (s, 1H), 7.56 (d, J = 7.7 Hz, 1H), 7.51 (d, J = 8.5 Hz, 2H), 7.45 (dd, J = 8.5, 2.2 Hz, 1H), 7.39 (s, 1H), 7.27 (d, J = 7.7 Hz, 1H), 7.16 (t, J = 7.7 Hz, 1H), 7.09 (d, J = 8.5 Hz, 2H), 6.79 (t, J = 5.9 Hz, 1H), 6.57 (d, J = 8.6 Hz, 1H), 4.39 (d, J = 5.9 Hz, 2H), 3.78 (s, 2H), 3.62 (s, 3H), 2.39 (s, 6H), 1.97 (s, 3H). ESMS: m/z 432 (M + H).

3-Chloro-*N*-[3-(4-dimethylaminomethyl-phenylcarbamoyl)-benzyl]-4-methoxy-benzamide (34). Yield 35%. ^{1}H NMR (400 MHz, $CDCl_3$) δ 9.18 (s, 1H), 7.89 (d, J = 2.2 Hz, 1H), 7.85 (s, 1H), 7.81−7.74 (m, 2H), 7.72 (d, J = 8.5 Hz, 2H), 7.49 (d, J = 7.7 Hz, 1H), 7.45 (t, J = 5.8 Hz, 1H), 7.38 (t, J = 7.7 Hz, 1H), 7.31 (d, J = 8.5 Hz, 2H), 6.91 (d, J = 8.7 Hz, 1H), 4.60 (d, J = 5.8 Hz, 2H), 4.03 (s, 2H), 3.93 (s, 3H), 2.65 (s, 6H). ESMS: m/z 452 (M + H).

***N*-[3-(4-Dimethylaminomethyl-phenylcarbamoyl)-benzyl]-4-methoxy-3-trifluoromethyl-benzamide (35).** Yield 26%. ^{1}H NMR (400 MHz, $CDCl_3$) δ 9.22 (s, 1H), 8.13 (d, J = 1.9 Hz, 1H), 8.10 (dd, J = 8.7, 2.1 Hz, 1H), 7.93 (s, 1H), 7.80 (d, J = 7.8 Hz, 1H), 7.74 (d, J = 8.5 Hz, 2H), 7.62 (t, J = 5.8 Hz, 1H), 7.53 (d, J = 7.6 Hz, 1H), 7.40 (t, J = 7.7 Hz, 1H), 7.32 (d, J = 8.4 Hz, 2H), 7.01 (d, J = 8.7 Hz, 1H), 4.65 (d, J = 5.8 Hz, 2H), 3.97 (s, 2H), 3.94 (s, 3H), 2.58 (s, 6H). ESMS: m/z 486 (M + H).

3-Chloro-*N*-[3-(4-dimethylaminomethyl-phenylcarbamoyl)-benzyl]-4-trifluoromethoxy-benzamide (36). Yield 30%. ^{1}H NMR (400 MHz, DMSO) δ 10.32 (s, 1H), 9.36 (t, J = 5.8 Hz, 1H), 8.21 (d, J = 2.0 Hz, 1H), 8.14 (s, 1H), 8.00 (dd, J = 8.6 Hz, 2.0 Hz, 1H), 7.89 (s, 1H), 7.85 (d, J = 7.4 Hz, 1H), 7.78−7.70 (m, 3H), 7.57−7.48 (m, 2H), 7.32 (d, J = 8.4 Hz, 1H), 4.58 (d, J = 5.8 Hz, 2H), 2.32 (s, 6H), buried CH_2. ESMS: m/z 506 (M + H).

4-Cyano-*N*-[3-(4-dimethylaminomethyl-phenylcarbamoyl)-benzyl]-benzamide (37). Yield 18%. ^{1}H NMR (400 MHz, $CDCl_3$) δ 8.83 (s, 1H), 7.99 (d, J = 8.6 Hz, 2H), 7.92 (s, 1H), 7.82 (d, J = 7.8 Hz, 1H), 7.79−7.69 (m, 4H), 7.57 (d, J = 7.8 Hz, 1H), 7.47 (t, J = 7.7 Hz, 1H), 7.42 (t, J = 5.9 Hz, 1H), 7.38 (d, J = 8.6 Hz, 2H), 4.71 (d, J = 5.8 Hz, 2H), 3.98 (s, 2H), 2.60 (s, 6H). ESMS: m/z 413 (M + H).

3-[3-(3-Cyano-phenyl)-ureidomethyl]-*N*-(2-piperidin-3-yl-ethyl)-benzamide (38). 3-Methoxycarbonyl-benzyl-ammonium chloride (111 mg, 0.55 mmol) was dissolved in DMF (2 mL) in a reaction vial. *Si*-DMA (570 mg, 0.85 mmol) was added, and the mixture was agitated for 1 h. Subsequently, *m*-cyanophenylisocyanate (72 mg, 0.5 mmol) was added and the mixture was agitated 16 h. SCX (114 mg, 0.1 mmol) was added and the mixture was agitated for 30 min. The solids were filtered and the solvent was concentrated to provide 3-[3-(3-cyano-phenyl)-ureidomethyl]-benzoic acid methyl ester: ESMS: m/z 310 (M + H). HPLC: 100%, which was used directly. The urea was dissolved in methanol (2 mL) and DMF (2 mL), and Amberlyst A26 (OH^- form) (746 mg, 1.0 mmol) was added. The resulting mixture was agitated for 16 h, and then the sorbent was filtered and washed with several portions of methanol. The product was eluted with formic acid (20% in methanol), and the eluent was concentrated to provide 3-[3-(3-cyano-phenyl)-ureidomethyl]-benzoic acid (85 mg, 58% yield). ^{1}H NMR (400 MHz, DMSO) δ 12.90 (br, 1H), 9.13 (s, 1H), 7.96 (t, J = 1.7 Hz, 1H), 7.90 (s, 1H), 7.83 (d, J = 7.6 Hz, 1H), 7.62 (d, J = 7.4 Hz, 1H), 7.55 (d, J = 7.7 Hz, 1H), 7.46 (d, J = 7.7 Hz, 1H), 7.44 (d, J = 8.2 Hz, 1H), 7.35 (d, J = 7.6 Hz, 1H), 7.04 (t, J = 5.9 Hz, 1H), 4.37 (d, J = 5.8 Hz, 2H). ESMS: m/z 296 (M + H). HPLC: 95%. This intermediate (29.5 mg, 0.1 mmol) and 3-(2-amino-ethyl)-piperidine-1-carboxylic acid *tert*-butyl ester (27.4 mg, 0.12 mmol) were coupled using the standard procedure with DIEA. The reaction mixture was purified directly by preparative HPLC using an acetonitrile/water/formic acid gradient to provide 3-(2-{3-[3-(3-cyano-phenyl)-ureidomethyl]-benzoylamino}-ethyl)-piperidine-1-carboxylic acid *tert*-butyl ester (36 mg, 71% yield). ESMS: m/z 506 (M + H). HPLC: 100%. This intermediate (36 mg, 0.07 mmol) was treated with 0.5 M HCl in dioxane (1 mL, 0.5 mmol). Methanol (0.5 mL) was added to solublize, and the resulting mixture was agitated for 1 h then concentrated. The isolate was purified by preparative HPLC using an acetonitrile/water/formic acid gradient providing the title compound (20 mg, 70% yield). ^{1}H NMR (400 MHz, DMSO) δ 9.96 (s, 1H), 8.53 (t, J = 5.6 Hz, 1H), 8.07−7.94 (m, 1H), 7.90−7.76 (m, 2H), 7.70 (d, J = 7.5 Hz, 1H), 7.65 (dq, J = 8.4, 1 Hz, 1H), 7.48−7.37 (m, 3H), 7.33−7.30 (m, 1H), 4.34 (d, J = 5.8 Hz, 2H), 3.49−3.27 (m, 2H), 3.19 (d, J = 13.0 Hz, 1H), 3.11 (d, J = 11.9 Hz, 1H), 2.75−2.61 (m, 1H), 2.55−2.45 (m, 1H), 1.84 (d, J = 14.6 Hz, 1H), 1.78−1.60 (m, 2H), 1.59−1.40 (m, 3H), 1.17−1.04 (m, 1H). ESMS: m/z 406 (M + H).

3-[3-(3,4-Dimethoxy-phenyl)-ureidomethyl]-*N*-(2-piperidin-3-yl-ethyl)-benzamide (39). 3-Methoxycarbonyl-benzyl-ammonium chloride (101 mg, 0.5 mmol) was dissolved in DMF (2 mL) in a reaction vial. *Si*-DMA (500 mg, 0.75 mmol) was added, and the mixture was agitated for 1 h. Subsequently, 3,4-dimethoxyphenylisocyanate (0.067 mL, 0.45 mmol) was added, and the mixture was agitated 16 h. SCX (100 mg, 0.09 mmol) was added, and the mixture was agitated for 15 min. The sorbents were filtered and washed with methanol and DMF, and the filtrate was concentrated to provide 3-[3-(3,4-dimethoxy-phenyl)-ureidomethyl]-benzoic acid methyl ester (155 mg, 90% yield). ESMS: m/z 345 (M + H). HPLC: 100%. The urea (110 mg, 0.32 mmol) was dissolved in DMF (1 mL), and Amberlyst A26 (OH^- form) (746 mg, 1.0 mmol) was added. The resulting mixture was agitated for 16 h. The sorbent was filtered and washed with several portions of DMF then methanol. The product was eluted with a solution of 20% formic acid in methanol, and the eluent was concentrated to provide 3-[3-(3,4-dimethoxyphenyl)-ureidomethyl]-benzoic acid (72 mg, 68% yield). ^{1}H NMR (400 MHz, DMSO) δ 13.00 (br, 1H), 8.48 (s, 1H), 7.88 (s, 1H), 7.80 (d, J = 7.6 Hz, 1H), 7.52 (d, J = 7.7 Hz, 1H), 7.44 (t, J = 7.6 Hz, 1H), 7.16 (s, 1H), 6.81 (s, 2H), 6.65 (t, J = 5.9 Hz, 1H), 4.33 (d, J = 5.8 Hz, 2H), 3.69 (s, 3H), 3.66 (s, 3H). ESMS: m/z 331 (M + H). HPLC: 100%. This intermediate (48 mg, 0.145 mmol) and 3-(2-amino-ethyl)-piperidine-1-carboxylic acid *tert*-butyl ester (34.3 mg, 0.15 mmol) were coupled using the standard procedure with NMM to provide 3-(2-{3-[3-(3,4-dimethoxy-phenyl)-ureidomethyl]-benzoylamino}-ethyl)-piperidine-1-carboxylic acid *tert*-butyl ester. ESMS: m/z 541 (M + H). HPLC: 100%, which was used directly. The intermediate was dissolved in DCM (1 mL) and treated with SCX (454 mg, 0.4 mmol), and the resulting mixture was agitated for 16 h. The mixture was filtered, and the sorbent was washed with several portions of DCM and methanol. The product was eluted with NH_3 (7N in methanol). The eluent was concentrated to provide the title compound (56 mg, 88% yield). ^{1}H NMR (400 MHz, DMSO) δ 8.53−8.39 (m, 2H), 7.77 (s, 1H), 7.70 (d, J = 5.3 Hz, 1H), 7.48−7.37 (m, 2H), 7.19 (s, 1H), 6.82 (s, 2H), 6.63 (t, J = 5.9 Hz, 1H), 4.33 (d, J = 5.7 Hz, 2H), 3.70 (s, 3H), 3.68 (s, 3H), 3.41−3.25 (m, 4H), 3.00 (d, J = 13.7 Hz, 2H), 1.68 (d, J = 13.7 Hz, 2H), 1.48−1.40 (m, 3H), 1.18−1.04 (m, 2H). ESMS: m/z 441 (M + H).

3-[3-(4-Cyano-phenyl)-ureidomethyl]-*N*-(2-piperidin-3-yl-ethyl)-benzamide (40). Common intermediate **54** (38.4 mg, 0.13 mmol) and 3-(2-amino-ethyl)-piperidine-1-carboxylic acid *tert*-butyl ester (34.3 mg, 0.15 mmol) were coupled using the standard procedure with DIEA. The reaction mixture was purified directly by preparative HPLC using an acetonitrile/water/formic acid gradient to provide 3-(2-{3-[3-(4-cyano-phenyl)-ureidomethyl]-benzoylamino}-ethyl)-piperidine-1-carboxylic acid *tert*-butyl ester (26 mg, 40% yield). ESMS: m/z 506 (M + H). HPLC: 100%. The intermediate (26 mg, 0.051 mmol) was treated with

0.5 M HCl in dioxane. Methanol (0.5 mL) was added to solublize, and the resulting mixture was agitated for 1 h then concentrated to provide the title compound, HCl salt (20.5 mg, 99% yield). ^{1}H NMR (400 MHz, DMSO) δ 9.63 (s, 1H), 8.82 (d, J = 10.4 Hz, 1H), 8.58−8.45 (m, 2H), 7.81 (s, 1H), 7.72 (d, J = 7.2 Hz, 1H), 7.65 (d, J = 8.7 Hz, 2H), 7.61 (d, J = 8.8 Hz, 2H), 7.49−7.39 (m, 2H), 7.18 (t, J = 5.8 Hz, 1H), 4.37 (d, J = 5.7 Hz, 2H), 3.40−3.09 (m, 5H), 2.74 (dd, J = 24.0, 11.2 Hz, 1H), 1.86 (d, J = 14.0 Hz, 1H), 1.80−1.70 (m, 2H), 1.65−1.37 (m, 3H), 1.14 (dd, J = 25.8, 11.0 Hz, 1H). ESMS: m/z 406 (M + H).

***N*-{3-[3-(4-Cyano-phenyl)-ureidomethyl]-phenyl}-3-piperidin-3-yl-propionamide (41).** 3-*t*-Butoxycarbonylamino-benzyl-ammonium chloride (103.5 mg, 0.4 mmol) was dissolved in DMF (1 mL) in a reaction vial, and *Si*-DMA (350 mg, 0.525 mmol) was added. The resulting mixture was agitated for 1 h, after which time *p*-cyanophenylisocyanate (52 mg, 0.36 mmol) was added and the reaction mixture was agitated 16 h. SCX (113 mg, 0.1 mmol) was added, and the mixture was agitated an additional 30 min. The reaction mixture was filtered and the sorbent was washed with DMF. The filtrate was concentrated to provide {3-[3-(4-cyano-phenyl)-ureidomethyl]-phenyl}-carbamic acid *tert*-butyl ester (140 mg, 95% yield). ESMS: m/z 367 (M + H). HPLC: 100%. The isolate was dissolved in DCM (5 mL) and treated with TFA (1 mL), and the resulting mixture was stirred at room temperature for 1.5 h. The solution was concentrated to provide 1-(3-amino-benzyl)-3-(4-cyano-phenyl)-urea (96 mg, 94% yield): ESMS: m/z 267 (M + H). HPLC: 94%. 3-(2-Carboxy-ethyl)-piperidine-1-carboxylic acid *tert*-butyl ester (38.6 mg, 0.15 mmol), and the urea prepared above (40 mg, 0.15 mmol) were coupled using the standard procedure with NMM to provide 3-(2-{3-[3-(4-cyano-phenyl)-ureidomethyl]-phenylcarbamoyl}-ethyl)-piperidine-1-carboxylic acid *tert*-butyl ester (63 mg, 83% yield). ESMS: m/z 506 (M + H). HPLC: 74%. This intermediate was dissolved in DCM (1 mL) and treated with SCX (341 mg, 0.3 mmol). The resulting mixture was agitated for 16 h. The mixture was filtered and the sorbent was washed with several portions of DCM and methanol. The product was eluted with NH_3 (7N in methanol). The eluent was concentrated and the isolate was purified by preparative HPLC using an acetonitrile/water/formic acid gradient providing the title compound (9 mg, 18% yield). ^{1}H NMR (400 MHz, DMSO) δ 9.97 (s, 1H), 9.95 (s, 1H), 7.76−7.59 (m, 5H), 7.53 (d, J = 8.1 Hz, 1H), 7.47 (s, 1H), 7.24 (t, J = 7.8 Hz, 1H), 6.96 (d, J = 7.6 Hz, 1H), 4.26 (d, J = 5.8 Hz, 2H), 3.16 (t, J = 12.5 Hz, 2H), 2.77−2.63 (m, 1H), 2.50−2.42 (m, 1H), 2.33 (t, J = 7.4 Hz, 2H), 1.82−1.71 (m, 2H), 1.65−1.45 (m 4H), 1.11 (dd, J = 22.9, 10.4 Hz, 1H). ESMS: m/z 406 (M + H).

3-[3-(4-Cyano-phenyl)-ureidomethyl]-*N*-(2-piperidin-4-yl-ethyl)-benzamide (42). Common intermediate **54** (30 mg, 0.10 mmol) and 4-(2-carboxy-ethyl)-piperidine-1-carboxylic acid *tert*-butyl ester (27.4 mg, 0.12 mmol) were coupled using the standard procedure with NMM to provide 4-(2-{3-[3-(4-cyano-phenyl)-ureidomethyl]-benzoylamino}-ethyl)-piperidine-1-carboxylic acid *tert*-butyl ester (50 mg, 97% yield). ESMS: m/z 506 (M + H); HPLC: 100%. This intermediate was dissolved in DCM (1 mL), and TFA (0.3 mL) was added. The resulting mixture was agitated for 2 h and then concentrated. The isolate was purified by preparative HPLC using an acetonitrile/water/formic acid gradient providing the title compound (37 mg, 91% yield). ^{1}H NMR (400 MHz, DMSO) δ 9.63 (s, 1H), 8.48 (t, J = 5.5 Hz, 1H), 7.78 (s, 1H), 7.75−7.57 (m, 5H), 7.49−7.34 (m, 3H), 4.35 (d, J = 5.8 Hz, 2H), 3.34−3.20 (m, 4H), 2.81 (dd, J = 14.0, 11.3 Hz, 2H), 1.85 (d, J = 12.6 Hz, 2H), 1.68−1.41 (m, 3H), 1.27 (dd, J = 23.4, 10.7 Hz, 2H). ESMS: m/z 406 (M + H).

3-[3-(4-Cyano-phenyl)-ureidomethyl]-*N*-(1,2,3,4-tetrahydro-isoquinolin-7-yl)-benzamide (43). Prepared according to the procedure used for the synthesis of **42**: 70% yield. ^{1}H NMR (400 MHz, DMSO) δ 10.29 (s, 1H), 9.47 (s, 1H), 7.88 (s, 1H), 7.83 (d, J = 8.6 Hz, 1H), 7.69−7.59 (m, 5H), 7.58−7.46 (m, 3H), 7.24 (t, J = 5.8 Hz, 1H), 7.16 (d, J = 8.4 Hz, 1H), 4.40 (d, J = 5.9 Hz, 2H), 4.17 (s, 2H), 3.31−3.21 (m, 2H), 2.88 (t, J = 5.5 Hz, 2H). ESMS: m/z 426 (M + H).

3-[3-(4-Cyano-phenyl)-ureidomethyl]-*N*-(4-dimethylaminomethyl-phenyl)-benzamide (44). Common intermediate **54** (23 mg, 0.078 mmol) and 4-dimethylaminomethylaniline (14.3 mg, 0.095 mmol) were coupled using the standard procedure with DIEA. The isolate was purified by preparative HPLC using an acetonitrile/water/formic acid gradient to provide the title compound (28 mg, 76% yield). ^{1}H NMR (400 MHz, DMSO) δ 10.10 (s, 1H), 9.17 (s, 1H), 7.70 (s, 1H), 7.66 (d, J = 7.0 Hz, 1H), 7.55 (d, J = 8.5 Hz, 2H), 7.50 (d, J = 8.9 Hz, 2H), 7.43 (d, J = 8.9 Hz, 2H), 7.37−7.29 (m, 2H), 7.10 (d, J = 8.5 Hz, 2H), 6.93 (t, J = 5.9 Hz, 1H), 4.23 (d, J = 5.9 Hz, 2H), 3.26 (s, 2H), 2.02 (s, 6H). ESMS: m/z 428 (M + H).

***N*-(4-Aminomethyl-phenyl)-3-[3-(4-cyano-phenyl)-ureidomethyl]-benzamide (45).** Prepared according to the procedure used for the synthesis of **42**: 85% yield. ^{1}H NMR (400 MHz, DMSO) δ 10.38 (s, 1H), 9.86 (s, 1H), 7.89 (s, 1H), 7.84 (d, J = 7.2 Hz, 1H), 7.79 (d, J = 8.5 Hz, 2H), 7.79−7.61 (m, 5H), 7.55−7.47 (m, 2H), 7.41 (d, J = 8.5 Hz, 2H), 4.40 (d, J = 5.8 Hz, 2H), 3.94 (s, 2H). ESMS: m/z 400 (M + H).

3-[3-(3-Chloro-4-cyano-phenyl)-ureidomethyl]-*N*-(3-dimethylaminomethyl-benzyl)-benzamide (46). 2-Chloro-4-aminobenzonitrile (305 mg, 2 mmol) and carbonyldiimidazole (324 mg, 2 mmol) were combined in a reaction vial, and DMF (5 mL) was added. The resulting mixture was heated at 60 °C for 16 h, and the product, 1,3-bis-(3-chloro-4-cyano-phenyl)-urea, was isolated by filtration and washed with several portions of 1N HCl (220 mg, 73% yield). ESMS: m/z 331 (M + H). HPLC: 100%. This intermediate (200 mg, 0.6 mmol) was dispersed in DMF (2 mL) in a microwave vial, and a solution of **53** (200 mg, 0.7 mmol), in DMF (1 mL), was added. The vial was sealed and heated in the microwave at 150 °C for 70 min. The reaction mixture was purified directly by preparative HPLC using an acetonitrile/water/formic acid gradient, then further purified by catch and release with Varian SCX cartridges to provide the title compound (60 mg, 18.4% yield). ^{1}H NMR (400 MHz, DMSO) δ 10.26 (s, 1H), 9.48 (s, 1H), 7.96−7.92 (m, 1H), 7.89−7.82 (m, 2H), 7.79 (d, J = 8.7 Hz, 1H), 7.72 (d, J = 8.4 Hz, 2H), 7.55−7.46 (m, 2H), 7.41 (dd, J = 8.7, 2.0 Hz, 1H), 7.26 (d, J = 8.4 Hz, 2H), 7.16 (t, J = 5.9 Hz, 1H), 4.41 (d, J = 5.9 Hz, 2H), 3.39 (s, 2H), 2.51 (s, 6H). ESMS: m/z 462 (M + H).

3-[3-(4-Amido-phenyl)-ureidomethyl]-*N*-(4-dimethylaminomethyl-phenyl)-benzamide (47). Compound **44** (20 mg, 0.058 mmol) was dissolved in 0.5 mL of 20% H_2SO_4 in TFA. The resulting mixture was agitated for 36 h. The reaction mixture was concentrated, and ice was added followed by 0.7 mL methanol and the mixture was purified directly by preparative HPLC using an acetonitrile/water/formic acid gradient providing the title compound (13 mg, 50% yield). ^{1}H NMR (400 MHz, DMSO) δ 10.29 (s, 1H), 8.95 (s, 1H), 8.16 (s, 1H), 7.88 (s, 1H), 7.84 (d, J = 7.0 Hz, 1H), 7.79−7.71 (m, 4H), 7.55−7.44 (m, 3H), 7.29 (d, J = 8.4 Hz, 2H), 7.15 (s, 1H), 6.89 (t, J = 5.8 Hz, 1H), 4.40 (d, J = 5.8 Hz, 2H), 3.50 (s, 2H), 2.24 (s, 6H). ESMS: m/z 446 (M + H).

3-[3-(3-Chloro-4-amido-phenyl)-ureidomethyl]-*N*-(4-dimethylaminomethyl-phenyl)-benzamide (48). Prepared from **46** according to the procedure used for the synthesis of **47**: 60% yield. ^{1}H NMR (400 MHz, DMSO) δ 10.30 (s, 1H), 8.99 (s, 1H), 7.88 (s, 1H), 7.84 (d, J = 7.0 Hz, 1H), 7.77 (d, J = 8.4 Hz, 2H), 7.72−7.66 (m, 2H), 7.57−7.47 (m, 2H), 7.41 (s, 1H), 7.37−7.31 (m, 3H), 7.26 (dd, J = 8.4, 1.9 Hz, 1H), 6.91 (t, J = 5.3 Hz, 1H), 4.40 (d, J = 5.8 Hz, 2H), 3.63 (s, 2H), 2.33 (s, 6H). ESMS: m/z 480 (M + H).

3-[3-(3-Amido-phenyl)-ureidomethyl]-*N*-(4-dimethylaminomethyl-phenyl)-benzamide (49). Intermediate **53** (36.8 mg, 0.13 mmol) was dissolved in DMF (1 mL) and 3-cyanophenylisocyanate (21.6 mg, 0.15 mmol) was added. The reaction mixture was agitated for 72 h then purified directly by preparative HPLC using an acetonitrile/water/formic acid gradient to provide

3-[3-(3-cyano-phenyl)-ureidomethyl]-*N*-(4-dimethylaminomethyl-phenyl)-benzamide (28 mg, 50.4% yield). This intermediate was then converted to the title compound according to the method described for the synthesis of **47**: 45% yield. ^{1}H NMR (400 MHz, DMSO) δ 10.29 (s, 1H), 8.80 (s, 1H), 7.91−7.81 (m, 4H), 7.75 (d, J = 8.5 Hz, 2H), 7.62 (d, J = 7.0 Hz, 1H), 7.55−7.47 (m, 2H), 7.39 (d, J = 7.7 Hz, 1H), 7.29 (d, J = 7.9 Hz, 4H), 6.81 (t, J = 6.0 Hz, 1H), 4.40 (d, J = 5.8 Hz, 2H), 3.52 (s, 2H), 2.25 (s, 6H). ESMS: m/z 446 (M + H).

3-[3-(4-Amido-phenyl)-ureidomethyl]-*N*-(1,2,3,4-tetrahydro-isoquinolin-7-yl)-benzamide (50). Prepared from **43** according to the procedure used for the synthesis of **47**: 72% yield. ^{1}H NMR (400 MHz, DMSO) δ 10.26 (s, 1H), 9.08 (s, 1H), 7.90 (s, 1H), 7.83 (d, J = 7.1 Hz, 1H), 7.80−7.73 (m, 3H), 7.59 (s, 1H), 7.56−7.43 (m, 5H), 7.19−7.08 (m, 2H), 7.03 (t, J = 5.8 Hz, 1H), 4.39 (d, J = 5.8 Hz, 2H), 4.04 (s, 2H), 3.14 (t, J = 5.8 Hz, 2H), 2.79 (t, J = 5.7 Hz, 2H). ESMS: m/z 444 (M + H).

ROCK1/ROCK 2 Dose−Response Assay. The activity of ROCK1 (1−477) and ROCK2 (1−543) kinases was measured utilizing Cambrex PKLight ATP detection reagent (Cambrex catalogue no. LT27-200), a homogeneous assay technology using luciferin-luciferase to quantify residual ATP. The assay was performed in 96-well half area, white, nonbinding surface microtiter plates (Corning, catalogue no. 3642) in assay buffer consisting of 25 mM HEPES (pH 7.5), 10 mM $MgCl_2$, 50 mM KCl, 0.2% BSA, 0.01% CHAPS, 100 μM Na_3VO_4, and 200 μM TCEP. Test compounds received as 5 mg/mL DMSO stocks were serially diluted 1:3 in DMSO for the 10-point concentration response. The DMSO dilutions were further diluted in the assay buffer, and 10 μL of this dilution was added to the assay plate, for a final starting assay concentration of 3 μg/mL in 1% DMSO. ROCK1 (12.6 μM stock) was diluted to 5 nM in assay buffer, and 30 μL was added to the assay, for a final concentration of 3 nM in a total volume of 30 μL. ROCK2 (29.0 μM stock) was diluted to 8.33 nM in assay buffer, and 30 μL was added to the assay for a final concentration of 5 nM in a total volume of 30 μL. After 15 min of preincubation of the test compounds with the kinase, a 10 μL volume of a mixture of 3.75 μM ATP, and 2.5 μM peptide substrate (AKRRRLSSLRA,[34a,34b] ANASPEC, catalogue no. 27192) diluted in assay buffer was added to each well for a final concentration of 750 nM ATP and 500 nM peptide. The kinase reaction mixture was incubated for 90 min at 28 °C. Following incubation, 30 μL of ATP detection reagent diluted in reconstitution buffer was added to the assay plates, and the resulting mixtures were incubated at room temperature for 15 min. The relative light unit (RLU) signal was measured on the Analyst plate reader (Molecular Devices) in luminescence mode. The RLU signals were converted to percent of control (POC) values using the formula POC = 100(BCTRL − Signal)/(BCTRL − PCTRL), where signal is the test well signal, BCTRL is the average of background (negative control) well signals on the plate, and PCTRL is the average of positive control well signals on the plate. For the concentration-responsive compounds, POC values as a function of test compound concentration were fitted to a four parameter logistic equation of the form: $y = A + (B - A)/[1 + (x/C)^D]$, where A, B, C, and D are fitted parameters (parameter B is fixed at zero POC) and x and y are the independent and dependent variables, respectively. The IC_{50} (50% inhibitory concentration) was determined as the inflection point parameter, C.

Rat Aortic Ring Assay. Segments of rat thoracic aorta were dissected from Sprague−Dawley rats cleaned of excess connective tissue and cut into 3−4 mm rings in a Petri dish filled with 4 °C PBS (phosphate buffer solution: NaCl (118 mM/L), KCl (4.7 mM/L), $CaCl_2$ (1.6 mM/L), KH_2PO_4 (1.2 mM/L), $MgCl_2$ (1.2 mM/L), dextrose (10 mM/L), $NaHCO_3$ (25 mM/L), NaEDTA (0.02 mM/L) at pH 7.25 and kept on ice before dissection. The rings were then suspended between two stainless steel wires, both of which were fixed to a stainless steel support rod on one side and the other side connected to a force transducer and placed into 37 °C temperature-controlled tissue baths containing PBS that was constantly oxygenated with 95% O_2 and 5% CO_2. Isometric force was continually measured and the data collected by a digital acquisition system. The rings were placed under a preload of 2.5g of force, which was continuously adjusted during a 1 h equilibration period to serve as baseline force. This amount of force was chosen from a series of preliminary force−force experiments, which showed near maximum contraction with 125 mM KCl. Rings were contracted with 50 mM KCL to obtain the maximum contraction level for normalization. Following a washout period of 30 min, the rings were preconstricted with 10^{-6} M phenylephrine and relaxed with a bolus dose of 10^{-7} M acetylcholine to check the integrity of the endothelium. Following a second washout period of 30 min, rings were preconstricted a second time with 10^{-6} M phenylephrine and the contraction allowed to stabilize. A cumulative dose response of a Rho-kinase inhibitor was tested in a DMSO vehicle at a 1:1000 dilution using half log intervals. After each dose of inhibitor, the response was allowed to stabilize before the addition of the next dose. Following the cumulative dose response with inhibitor, the tissues were washed 3× in PBS and allowed to equilibrate at resting tension. A second KCL contraction was performed as stated above to check the viability of the tissue. Following this, a second phenylephrine contraction and acetylcholine bolus dose were given as above to check for the integrity of the endothelium following inhibitor testing. The effect of the Rho-kinase inhibitors were expressed as a percentage relaxation from the phenylephrine-induced contraction at each dose. The IC_{50} for each inhibitor was determined from the concentration that produced 50% relaxation from the phenylephrine-induced contraction. The data for each inhibitor represents the mean from four different segments from four different rats.

Acknowledgment. We thank Rachel Kroe-Barrett for the ITC experiments.

Supporting Information Available: ATP competition studies, data comparison for luciferase inhibitors using IMAP and luciferase assay formats, IMAP dose−response assay method, additional kinase selectivity data, and target independent profiling methods. This material is available free of charge via the Internet at http://pubs.acs.org.

References

(1) Sams-Dodd, F. Target-based drug discovery: is something wrong? *Drug Discovery Today: Targets* **2005**, *10*, 139–147.

(2) (a) Davis, A. M.; Keeling, D. J.; Steele, J.; Tomkinson, N. P.; Tinker, A. C. Components of successful lead generation. *Curr. Top. Med. Chem.* **2005**, *5*, 421–439. (b) Alanine, A.; Nettekoven, M.; Roberts, E.; Thomas, A. W. Lead generation—enhancing the success of drug discovery by investing in the hit to lead process. *Comb. Chem. High Throughput Screening* **2003**, *6*, 51–66. (c) Bleicher, K. H.; Nettekoven, M.; Peters, J.-U.; Wyler, R. Lead generation: sowing the seeds for future success. *Chimia* **2004**, *58*, 588–600. (d) Michne, W. F. Hit-to-lead chemistry: A key element in new lead generation. *Pharm. News* **1996**, *3*, 19–21.

(3) Boureux, A; Vignal, E; Faure, S; Fort, P. Evolution of the Rho family of ras-like GTPases in eukaryotes. *Mol. Biol. Evol.* **2007**, *24* (1), 203–16.

(4) (a) Lai, A.; Frishman, W. H. Rho-kinase inhibition in the therapy of cardiovascular disease. *Cardiol. Rev.* **2005**, *13*, 285–292. (b) Hu, E.; Lee, D. Rho kinase as potential therapeutic target for cardiovascular diseases: opportunities and challenges. *Expert Opin. Ther. Targets* **2005**, *9*, 715–736.

(5) (a) Takai, Y.; Sasaki, T.; Matozaki, T. Small GTP-binding proteins. *Physiol. Rev.* **2001**, *81*, 153–208. (b) Fukata, M.; Kaibuchi, K. Rho-family GTPases in cadherin-mediated cell−cell adhesion. *Nat. Rev. Mol. Cell. Biol.* **2001**, *2*, 887–897. (c) Ridley, A. J. Rho family proteins: coordinating cell responses. *Trends Cell Biol.* **2001**, *11*, 471–477.

(6) (a) Shimokawa, H.; Rashid, M. Development of Rho-kinase inhibitors for cardiovascular medicine. *Trends Pharmacol. Sci.* **2007**, *28*, 296–302. (b) Loirand, G.; Guérin, P.; Pacaud, P. Rho Kinases in cardiovascular physiology and pathophysiology. *Circ. Res.* **2006**, *98*, 322–334.
(7) Trauger, J. W.; Lin, F.-F.; Turner, M. S.; Stephens, J.; LoGrasso, P. V. Kinetic mechanism for human Rho-Kinase II (ROCK-II). *Biochemistry* **2002**, *41*, 8948–8953.
(8) Leung, T.; Chen, X.-Q.; Manser, E.; Lim, L. The p160 RhoA-binding kinase ROKα is a member of a kinase family and is involved in the reorganization of the cytoskeleton. *Mol. Cell. Biol.* **1996**, *16*, 5313–5327.
(9) Yoneda, A.; Multhaupt, H. A. B.; Couchman, J. R. The Rho kinases I and II regulate different aspects of myosin II activity. *J. Cell Biol.* **2005**, *170*, 443−453, and references cited therein.
(10) Riento, K.; Totty, N.; Villalonga, P.; Garg, R.; Guasch, R.; Ridley, A. J. RhoE function is regulated by ROCK I-mediated phosphorylation. *EMBO J.* **2005**, *24*, 1170–1180.
(11) Rubenstein, N. M.; Callahan, J. A.; Lo, D. H.; Firestone, G. L. Selective glucocorticoid control of Rho kinase isoforms regulate cell−cell interactions. *Biochem. Biophys. Res. Commun.* **2007**, *354*, 603–607.
(12) (a) Wettschureck, N.; Offermanns, S. Rho/Rho-kinase mediated signaling in physiology and pathophysiology. *J. Mol. Med.* **2002**, *80*, 629–638. (b) Amano, M.; Ito, M.; Kimura, K.; Fukata, Y.; Chihara, K.; Nakano, T.; Matsuura, Y.; Kaibuchi, K. Phosphorylation and activation of myosin by Rho-associated kinase (Rho-kinase). *J. Biol. Chem.* **1996**, *271*, 20246–20249.
(13) (a) Feng, J.; Ito, M.; Kureishi, Y.; Ichikawa, K.; Amano, M.; Isaka, N.; Okawa, K.; Iwamatsu, A.; Kaibuchi, K.; Hartshorne, D. J.; Nakano, T. Rho-associated kinase of chicken gizzard smooth muscle. *J. Biol. Chem.* **1999**, *274*, 3744–3752. (b) Fu, X.; Gong, M. C.; Jia, T.; Somlyo, A. V.; Somlyo, A. P. The effects of the Rho-kinase inhibitor Y-27632 on arachidonic acid-, GTPgammaS-, and phorbol ester-induced Ca^{2+}-sensitization of smooth muscle. *FEBS Lett.* **1998**, *440*, 183–187.
(14) Budzyn, K.; Marley, P. D.; Sobey, C. G. Targeting Rho and Rho-kinase in the treatment of cardiovascular disease. *Trends Pharmacol. Sci.* **2006**, *27*, 97–104.
(15) (a) Mueller, B. K.; Mack, H.; Teusch, N. Rho kinase, a promising drug target for neurological disorders. *Nat. Rev. Drug Discovery* **2005**, *4*, 387–398. (b) Chrissobolis, S.; Sobey, C. G. Recent evidence for an involvement of Rho-kinase in cerebral vascular disease. *Stroke* **2006**, *37*, 2174–2180.
(16) Ohnaka, K.; Shimoda, S.; Nawata, H.; Shimokawa, H.; Kaibuchi, K.; Iwamoto, Y.; Takayanagi, R. Pitavastatin enhanced BMP-2 and osteocalcin expression by inhibition of Rho-associated kinase in human osteoblasts. *Biochem. Biophys. Res. Commun.* **2001**, *287*, 337–342.
(17) (a) Yin, L.; Morishige, K.; Takahashi, T.; Hashimoto, K.; Ogata, S.; Tsutsumi, S.; Takata, K.; Ohta, T.; Kawagoe, J.; Takahashi, K.; Kurachi, H. Fasudil inhibits vascular endothelial growth factor-induced angiogenesis in vitro and in vivo. *Mol. Cancer Ther.* **2007**, *6*, 1517–1525. (b) Rattan, R.; Giri, S.; Singh, A. K.; Singh, I. Rho/ROCK pathway as a target of tumor therapy. *J. Neurosci. Res.* **2006**, *83*, 243–255.
(18) Kobayashi, M.; Kume, H.; Oguma, T.; Makino, Y.; Ito, Y.; Shimokata, K. Mast cell tryptase causes homologous desensitization of β-adrenoceptors by Ca^{2+} sensitization in tracheal smooth muscle. *Clin. Exp. Allergy* **2008**, *38*, 135–144.
(19) Rao, V. P.; Epstein, D. L. Rho GTPase/Rho kinase inhibition as a novel target for the treatment of glaucoma. *BioDrugs* **2007**, *21*, 167–177. Tokushige, H.; Inatani, M.; Nemoto, S.; Sakaki, H.; Katayama, K.; Uehata, M.; Tanihara, H. Effects of topical administration of Y-39983, a selective Rho-associated protein kinase inhibitor, on ocular tissues in rabbits and monkeys. *Invest. Ophthalmol. Visualization Sci.* **2007**, *48*, 3216–2322.
(20) Shimokawa, H.; Takeshita, A. Rho-kinase is an important therapeutic target in cardiovascular medicine. *Arterioscler. Thromb. Vasc. Biol.* **2005**, *25*, 1767–1775.
(21) Budzyn, K.; Sobey, C. G. Vascular rho kinases and their potential therapeutic applications. *Curr. Opin. Drug Discovery Dev.* **2007**, *10*, 590–596.
(22) Viswambharan, H.; Ming, X.-F.; Zhu, S.; Hubsch, A.; Lerch, P.; Vergères, G.; Rusconi, S.; Yang, Z. Reconstituted high-density lipoprotein inhibits thrombin-induced endothelial tissue factor expression through inhibition of RhoA and stimulation of phosphatidylinositol 3-kinase but not Akt/endothelial nitric oxide synthase. *Circ. Res.* **2004**, *94*, 918–925.
(23) (a) McKinsey, T. A.; Kass, D. A. Small-molecule therapies for cardiac hypertrophy: moving beneath the cell surface. *Nat. Rev. Drug Discovery* **2007**, *6*, 617–635. (b) Jain, M. K.; Ridker, P. M. Anti-inflammatory effects of statins: clinical evidence and basic mechanisms. *Nat. Rev. Drug Discovery* **2005**, *4*, 977–987.
(24) (a) Stavenger, R. A. Rho-kinase inhibitors for cardiovascular disease. *Annu. Rep. Med. Chem.* **2008**, *43*, 87–102. (b) Takami, A.; Iwakubo, M.; Okada, Y.; Kawata, T.; Odai, H.; Takahashi, N.; Shindo, K.; Kimura, K.; Tagami, Y.; Miyake, M.; Fukushima, K.; Inagaki, M.; Amano, M.; Kaibuchi, K.; Iijima, H. Design and synthesis of Rho kinase inhibitors (I). *Bioorg. Med. Chem.* **2004**, *12*, 2115–2137. (c) Goodman, K. B.; Cui, H.; Dowdell, S. E.; Gaitanopoulos, D. E.; Ivy, R. L.; Sehon, C. A.; Stavenger, R. A.; Wang, G. Z.; Viet, A. Q.; Xu, W.; Ye, G.; Semus, S. F.; Evans, C.; Fries, H. E.; Jolivette, L. J.; Kirkpatrick, R. B.; Dul, E.; Khandekar, S. S.; Yi, T.; Jung, D. K.; Wright, L. L.; Smith, G. K.; Behm, D. J.; Bentley, R.; Doe, C. P.; Hu, E.; Lee, D. Development of dihydropyridone indazole amides as selective Rho-kinase inhibitors. *J. Med. Chem.* **2007**, *50*, 6–9. (d) Stavenger, R. A.; Cui, H.; Dowdell, S. E.; Franz, R. G.; Gaitanopoulos, D. E.; Goodman, K. B.; Hilfiker, M. A.; Ivy, R. L.; Leber, J. D.; Marino, J. P.; Oh, H.-J.; Viet, A. Q.; Xu, W.; Ye, G.; Zhang, D.; Zhao, Y.; Jolivette, L. J.; Head, M. S.; Semus, S. F.; Elkins, P. A.; Kirkpatrick, R. B.; Dul, E.; Khandekar, S. S.; Yi, T.; Jung, D. K.; Wright, L. L.; Smith, G. K.; Behm, D. J.; Doe, C. P.; Bentley, R.; Chen, Z. X.; Hu, E.; Lee, D. Discovery of aminofurazan-azabenzimidazoles as inhibitors of Rho-kinase with high kinase selectivity and antihypertensive activity. *J. Med. Chem.* **2007**, *50*, 2–5. (e) Sehon, C. A.; Wang, G. Z.; Viet, A. Q.; Goodman, K. B.; Dowdell, S. E.; Elkins, P. A.; Semus, S. F.; Evans, C.; Jolivette, L. J.; Kirkpatrick, R. B.; Dul, E.; Khandekar, S. S.; Yi, T.; Wright, L. L.; Smith, G. K.; Behm, D. J.; Bentley, R.; Doe, C. P.; Hu, E.; Lee, D. Potent, selective and orally bioavailable dihydropyrimidine inhibitors of Rho kinase (ROCK1) as potential therapeutic agents for cardiovascular diseases. *J. Med. Chem.* **2008**, *51*, 6631–6634. (f) Feng, Y.; Yin, Y.; Weiser, A.; Griffin, E.; Cameron, M. D.; Lin, L.; Ruiz, C.; Schürer, S. C.; Inoue, T.; Rao, P. V.; Schröter, T.; LoGrasso, P. Discovery of substituted 4-(pyrazol-4-yl)-phenylbenzodioxane-2-carboxamides as potent and highly selective Rho kinase (ROCK-II) inhibitors. *J. Med. Chem.* **2008**, *51*, 6642–6645.
(25) Liao, J. K.; Seto, M.; Noma, K. J. Rho kinase (ROCK) inhibitors. *J. Cardiovasc. Pharmacol.* **2007**, *50*, 17–24.
(26) (a) Jacobs, M.; Hayakawa, K.; Swenson, L.; Bellon, S.; Fleming, M.; Taslimi, P.; Doran, J. The structure of dimeric ROCK I reveals the mechanism for ligand selectivity. *J. Biol. Chem.* **2006**, *281*, 260–268. (b) Yamaguchi, H.; Miwa, Y.; Kasa, M.; Kitano, K.; Amano, M.; Kaibuchi, K.; Hakoshima, T. Structural basis for induced-fit binding of Rho-kinase to the inhibitor Y-27632. *J. Biochem.* **2006**, *140*, 305–311. (c) Yamaguchi, H.; Kasa, M.; K.; Amano, M.; Kaibuchi, K.; Hakoshima, T. Molecular mechanism for the regulation of Rho-kinase by dimerization and its inhibition by fasudil. *Structure* **2006**, *14*, 589–600.
(27) Morwick, T. M.; Berry, A.; Brickwood, J.; Cardozo, M.; Catron, K.; DeTuri, M.; Emeigh, J.; Homon, C.; Hrapchak, M.; Jacober, S.; Jakes, S.; Kaplita, P.; Kelly, T.; Ksiazek, J.; Liuzzi, M.; Magolda, R.; Mao, C.; Marshall, D.; McNeil, D.; Prokopowicz, A. III; Sarko, C.; Scouten, E.; Sledziona, C.; Sun, S.; Watrous, J.; Wu, J.-P.; Cywin, C. L. Evolution of the thienopyridine class of inhibitors of IκB kinase-β: Part I—hit-to-lead strategies. *J. Med. Chem.* **2006**, *49*, 2898–2908.
(28) Breitenlechner, C.; Gassel, M.; Hidaka, H.; Kinzel, V.; Huber, R.; Engh, R. A.; Bossemeyer, D. Protein Kinase A in Complex with Rho-Kinase Inhibitors Y-27632, Fasudil, and H-1152P: Structural Basis of Selectivity. *Structure* **2003**, *11*, 1595–1607.
(29) Auld, D. S.; Southall, N. T.; Jadhav, A.; Johnson, R. L.; Diller, D. J.; Simeonov, A.; Austin, C. P.; Inglese, J. Characterization of chemical libraries for luciferase inhibitory activity. *J. Med. Chem.* **2008**, *51*, 2372–2386.See also: Auld, D. S.; Zhang, Y.-Q.; Southall, N. T.; Rai, G.; Landsman, M.; MacLure, J.; Langevin, D.; Thomas, C. J.; Austin, C. P.; Inglese, J. A basis for reduced chemical library inhibition of firefly luciferase obtained from directed evolution. *J. Med. Chem.* **2009**, *52*, 1450−1458 for a comparison of assay reagents.
(30) (a) Morwick, T. M. High-throughput ester hydrolysis with catch-and-release isolation of carboxylic acids. *J. Comb. Chem.* **2006**, *8*, 649–651. (b) Liu, Y.-S.; Zhao, C.; Bergbreiter, D. E.; Romo, D. Simultaneous deprotection and purification of BOC-amines based on ionic resin capture. *J. Org. Chem.* **1998**, *63*, 3471.
(31) Moore, M. L. The Leukart Reaction. *Org. React.* **1941**, *5*, 301–330.
(32) Riley, R. J.; Parker, A. J.; Trigg, S.; Manners, C. N. Development of a generalized, quantitative physiochemical model of CYP3A4 inhibition for use in early drug discovery. *Pharm. Res.* **2001**, *18*, 652–655.
(33) Doe, C.; Bentley, R.; Behm, D. J.; Lafferty, R.; Stavenger, R.; Jung, D.; Bamford, M.; Panchal, T.; Grygielko, E.; Wright, L. L.; Smith, G. K.; Chen, Z.; Webb, C.; Khandekar, S.; Yi, T.; Kirkpatrick, R.; Dul, E.; Jolivette, L.; Marino, J. P., Jr.; Willette, R.; Lee, D.; Hu, E. Novel Rho kinase inhibitors with anti-inflammatory and vasodilatory activities. *J. Pharmacol. Exp. Ther.* **2007**, *320*, 89–98.

(34) (a) Turner, M. S.; Lin, F.-F.; Trauger, J. W.; Stephens, J.; LoGrasso, P. L. Characterization and purification of truncated human Rho-kinase II expressed in *Sf*-21 cells. *Arch. Biochem. Biophys.* **2002**, *405*, 13–20. (b) Khandekar, S. S.; Yi, T.; Dul, E.; Wright, L. L.; Chen, S.; Scott, G. F.; Smith, G. K.; Lee, D.; Hu, E.; Kirkpatrick, R. B. Expression, purification, and characterization of an enzymatically active truncated human Rho-kinase I (ROCK I) domain expressed in Sf-9 insect cells. *Protein Pept. Lett.* **2006**, *13*, 369–376. (c) Knight, Z. A.; Shokat, K. M. Features of selective kinase inhibitors. *Chem. Biol.* **2005**, *12*, 621–637.